*International Tables for Crystallography* (2006). Vol. C, Chapter 8.7, pp. 713–734.

# 8.7. Analysis of charge and spin densities

By P. Coppens, Z. Su and P. J. Becker

## 8.7.1. Outline of this chapter

Knowledge of the electron distribution is crucial for our understanding of chemical and physical phenomena. It has been assumed in many calculations (*e.g.* Thomas, 1926; Fermi, 1928; and others), and formally proven for non-degenerate systems (Hohenberg & Kohn, 1964) that the electronic energy is a functional of the electron density. Thus, the experimental measurement of electron densities is important for our understanding of the properties of atoms, molecules and solids. One of the main methods to achieve this goal is the use of scattering techniques, including elastic X-ray scattering, Compton scattering of X-rays, magnetic scattering of neutrons and X-rays, and electron diffraction.

Meaningful information can only be obtained with data of the utmost accuracy, which excludes most routinely collected crystallographic data sets. The present chapter will review the basic concepts and expressions used in the interpretation of accurate data in terms of the charge and spin distributions of the electrons. The structure-factor formalism has been treated in Chapter 1.2 of Volume B (*IT*B, 1992).

## 8.7.2. Electron densities and the *n*-particle wavefunction

A wavefunction $\psi(1, 2, 3, \ldots, n)$ for a system of $n$ electrons is a function of the $3n$ space and $n$ spin coordinates of the electrons. The wavefunction must be antisymmetric with respect to the interchange of any two electrons. The most general density function is the $n$-particle density matrix, of dimension $4n \times 4n$, defined as

$$\Gamma^n(1, 2, \ldots, n; 1', 2', \ldots, n') = \psi(1, 2, \ldots, n)\psi^*(1', 2', \ldots, n'). \quad (8.7.2.1)$$

In this expression, each index represents both the continuous space coordinates and the discontinuous spin coordinates of each of the $n$ particles. Thus, the $n$-particle density matrix is a representation of the state in a $6n$-dimensional coordinate space, and the $n$-dimensional (discontinuous) spin state.

The *pth reduced density matrix* can be derived from (8.7.2.1) by integration over the space and spin coordinates of $n - p$ particles,

$$\Gamma^p(1, 2, \ldots, p; 1', 2', \ldots, p') = \binom{n}{p} \int \Gamma^n(1, 2, \ldots, p, p+1, \ldots, n; 1', 2', \ldots, p', p+1, \ldots, n)\, \mathrm{d}(p+1) \ldots \mathrm{d}n. \quad (8.7.2.2)$$

According to a basic postulate of quantum mechanics, physical properties are represented by their expectation values $\langle F \rangle$ obtained from the corresponding *operator equation*,

$$\langle F \rangle = \langle \psi | \widehat{F} | \psi \rangle / \langle \psi | \psi \rangle, \quad (8.7.2.3)$$

where $\widehat{F}$ is a (Hermitian) operator. As almost all operators of interest are one- or two-particle operators, the one- and two-particle matrices $\Gamma^1(1\ ;1')$ and $\Gamma^2(1, 2\ ;1', 2')$ are of prime interest. The charge density, or *one-electron density*, can be obtained from $\Gamma^1(1; 1')$ by setting $1' = 1$ and integrating over the spin coordinates, *i.e.*

$$\rho(\mathbf{r}) = n \int \Gamma^1(1, 1)\, \mathrm{d}s_1 = n \int \psi(1, 2, \ldots, n)\psi^*(1, 2, \ldots, n)\, \mathrm{d}s_1\, \mathrm{d}2 \ldots \mathrm{d}n. \quad (8.7.2.4)$$

An electron density $\rho(\mathbf{r})$ that can be represented by an antisymmetric $N$-electron wave function and is derivable from that wave function through (8.7.2.4) is called $N$-representable. As in any real system, the particles will undergo vibrations, so (8.7.2.4) must be modified to allow for the continuous change in the configuration of the nuclei. The commonly used Born–Oppenheimer approximation assumes that the electrons rearrange instantaneously in the field of the oscillating nuclei, which leads to the separation

$$\psi = \psi_e(\mathbf{r}, \mathbf{R}) \cdot \psi_N(\mathbf{R}), \quad (8.7.2.5)$$

where $\mathbf{r}$ and $\mathbf{R}$ represent the electronic and nuclear coordinates, respectively, and $\psi_e$ is the electronic wavefunction, which is a function of both the electronic and nuclear coordinates. The time-averaged, one-electron density $\langle \rho(\mathbf{r}) \rangle$, which is accessible experimentally through the elastic X-ray scattering experiment, is obtained from the static density by integration over all nuclear configurations:

$$\langle \rho(\mathbf{r}) \rangle = \int \rho(\mathbf{r}, \mathbf{R}) P(\mathbf{R})\, \mathrm{d}\mathbf{R}, \quad (8.7.2.6)$$

where $P(\mathbf{R})$ is the normalized probability distribution function of the nuclear configuration $\mathbf{R}$. The total X-ray scattering can be derived from the two-particle matrix $\Gamma(1, 2, 1', 2')$ through use of the two-particle scattering operator. The total X-ray scattering includes the inelastic incoherent Compton scattering, which is related to the momentum density $\pi(\mathbf{p})$.

The wavefunction in momentum space, defined by the coordinates $\widehat{\mathbf{J}} = \widehat{p}_j, s_j$ of the $j$th particle (here the caret indicates momentum-space coordinates), is given by the Dirac–Fourier transform of $\psi$,

$$\widehat{\psi}(\widehat{1}, \widehat{2}, \ldots, \widehat{n}) = (2\pi\hbar)^{-3n/2} \int \psi(1, 2, \ldots, n) \times \exp\left(-i/\hbar \sum_j \mathbf{p}_j \cdot \mathbf{r}_j\right) \mathrm{d}\mathbf{r}_1\, \mathrm{d}\mathbf{r}_2 \ldots \mathrm{d}\mathbf{r}_n, \quad (8.7.2.7)$$

leading, in analogy to (8.7.2.2), to the one-electron density matrix

$$\pi^1(\widehat{1}, \widehat{1}') = n \int \psi(\widehat{1}, \widehat{2}, \ldots, \widehat{n})\psi^*(\widehat{1}, \widehat{2}, \ldots, \widehat{n})\, \mathrm{d}\widehat{2} \ldots \mathrm{d}\widehat{n}, \quad (8.7.2.8)$$

and the *momentum density*

$$\pi(p) = \int \pi^1(\widehat{1}, \widehat{1})\, \mathrm{d}s_1. \quad (8.7.2.9)$$

The *spin density distribution* of the electrons, $s(\mathbf{r})$, can be obtained from $\Gamma^1(1, 1')$ by use of the operator for the $z$ component of the spin angular momentum. If

$$s(\mathbf{r}, \mathbf{r}') = (2M)^{-1} \int s_z(1)\Gamma(1, 1')\, \mathrm{d}s_1, \quad s(\mathbf{r}) = s(\mathbf{r}, \mathbf{r}), \quad (8.7.2.10)$$

where $M$, the total magnetization, is the eigenvalue of the operator

$$S_z = \sum_i s_z(i).$$

## 8.7.3. Charge densities

### 8.7.3.1. *Introduction*

The charge density is related to the elastic X-ray scattering amplitude $F(\mathbf{S})$ by the expression

$$\langle \rho(\mathbf{r}) \rangle = \int F(\mathbf{S}) \exp(-2\pi i \mathbf{S} \cdot \mathbf{r}) \, \mathrm{d}\mathbf{S}, \tag{8.7.3.1}$$

or, for scattering by a periodic lattice,

$$\langle \rho(\mathbf{r}) \rangle = \frac{1}{V} \sum_{\mathbf{h}} F(\mathbf{h}) \exp(-2\pi i \mathbf{h} \cdot \mathbf{r}).$$

As $F(\mathbf{h})$ is in general complex, the Fourier transform (8.7.3.1) requires calculation of the phases from a model for the charge distribution. In the centrosymmetric case, the free-atom model is in general adequate for calculation of the signs of $F(\mathbf{h})$. However, for non-centrosymmetric structures in which phases are continuously variable, it is necessary to incorporate deviations from the free-atom density in the model to obtain estimates of the experimental phases.

Since the total density is dominated by the core distribution, differences between the total density $\rho(\mathbf{r})$ and reference densities are important. The reference densities represent hypothetical states without chemical bonding or with only partial chemical bonding. Deviations from spherical, free-atom symmetry are obtained when the reference state is the *promolecule*, the superposition of free-space spherical atoms centred at the nuclear positions. This difference function is referred to as the *deformation* density (or standard deformation density)

$$\Delta\rho(\mathbf{r}) = \rho(\mathbf{r}) - \rho_p(\mathbf{r}), \tag{8.7.3.2}$$

where $\rho_p(\mathbf{r})$ is the promolecule density. In analogy to (8.7.3.1), the deformation density may be obtained from

$$\langle \Delta\rho(\mathbf{r}) \rangle = \frac{1}{V} \sum \left[ F_{\mathrm{obs}}(\mathbf{h}) - F_{\mathrm{calc,free\ atom}}(\mathbf{h}) \right] \exp(-2\pi i \mathbf{h} \cdot \mathbf{r}), \tag{8.7.3.3}$$

where $F_{\mathrm{obs}}$ and $F_{\mathrm{calc}}$ are in general complex.

Several other different density functions analogous to (8.7.3.3), summarized in Table 8.7.3.1, may be defined. Particularly useful for the analysis of effects of chemical bonding is the fragment deformation density, in which a chemical fragment is subtracted from the total density of a molecule. The fragment density is calculated theoretically and thermally smeared before subtraction from an experimental density. 'Prepared' atoms rather than spherical atoms may be used as a reference state to emphasize the electron-density shift due to covalent bond formation.

Table 8.7.3.1. *Definition of difference density functions*

$$\Delta\rho = \frac{2}{V} \left\{ \sum_{0}^{1/2} (A_1 - A_2) \cos 2\pi \mathbf{h} \cdot \mathbf{r} + \sum_{0}^{1/2} (B_1 - B_2) \sin 2\pi \mathbf{h} \cdot \mathbf{r} \right\}$$

with $F = A + iB$.

| | |
|---|---|
| (*a*) Residual map | $A_1$, $B_1$ from observations calculated with model phases.<br>$A_2$, $B_2$ from refinement model. |
| (*b*) $X - X$ deformation map | $A_1$, $B_1$ from observation, with model phases.<br>$A_2$, $B_2$ from high-order refinement, free-atom model, or other reference state. |
| (*c*) $X - N$ deformation map [as (*b*) but] | $A_2$, $B_2$ calculated with neutron parameters. |
| (*d*) $X - (X + N)$ deformation map [as (*b*) but] | $A_2$, $B_2$ calculated with parameters from joint refinement of X-ray neutron data. |
| (*e*) $X - X$, $X - N$, $X - (X + N)$ valence map | As (*b*), (*c*), (*d*) with $A_1$, $B_1$ calculated with core-electron contribution only. |
| (*f*) Dynamic model map | $A_1$, $B_1$ from model.<br>$A_2$, $B_2$ with parameters from model refinement and free-atom functions. |
| (*g*) Static model map | $\rho_{\mathrm{model}} - \rho_{\mathrm{free\ atom}}$, where $\rho_{\mathrm{model}}$ is sum of static model density functions. |

### 8.7.3.2. *Modelling of the charge density*

The electron density $\rho(\mathbf{r})$ in the structure-factor expression

$$F_{\mathrm{calc}}(\mathbf{h}) \int_{\text{unit cell}} \rho(\mathbf{r}) \exp(2\pi i \mathbf{h} \cdot \mathbf{r}) \, \mathrm{d}\mathbf{r} \tag{8.7.3.4a}$$

can be approximated by a sum of non-normalized density functions $g_i(\mathbf{r})$ with scattering factor $f_i(\mathbf{h})$ centred at $\mathbf{r}_i$,

$$\rho(\mathbf{r}) = \sum_i g_i(\mathbf{r}) * \delta(\mathbf{r} - \mathbf{r}_i). \tag{8.7.3.5}$$

Substitution in (8.7.3.4*a*) gives

$$F(\mathbf{h}) = \sum_i f_i(\mathbf{h}) \exp(2\pi i \mathbf{h} \cdot \mathbf{r}_i). \tag{8.7.3.4b}$$

When $g_i(\mathbf{r})$ is the spherically averaged, free-atom density, (8.7.3.4*b*) represents the free-atom model. A distinction is often made between *atom-centred* models, in which all functions $g(\mathbf{r})$ are centred at the nuclear positions, and models in which additional functions are centred at other locations, such as in bonds or lone-pair regions.

A simple, atom-centred model with spherical functions $g(\mathbf{r})$ is defined by

$$\rho_{\mathrm{atom}}(\mathbf{r}) = P_{\mathrm{core}} \rho_{\mathrm{core}}(\mathbf{r}) + \kappa^3 P_{\mathrm{valence}} \rho_{\mathrm{valence}}(\kappa \mathbf{r}). \tag{8.7.3.6}$$

This 'kappa model' allows for charge transfer between atomic valence shells through the population parameter $P_{\mathrm{valence}}$, and for a change in nuclear screening with electron population, through the parameter $\kappa$, which represents an expansion ($\kappa < 1$), or a contraction ($\kappa > 1$) of the radial density distribution.

The atom-centred, spherical harmonic expansion of the electronic part of the charge distribution is defined by

$$\rho_{\mathrm{atom}}(\mathbf{r}) = P_{\mathrm{c}} \rho_{\mathrm{core}}(\mathbf{r}) + P_{\mathrm{v}} \kappa^3 \rho_{\mathrm{valence}}(\kappa r) + \sum_{l=0}^{l(\max)} \kappa'^3 R_l(\kappa' \zeta r) \sum_{m=0}^{l} \sum_{p} P_{lmp} d_{lmp}(\theta, \varphi), \tag{8.7.3.7}$$

where $p = \pm$ when $m$ is larger than 0, and $R_l(\kappa' \zeta r)$ is a radial function.

The real spherical harmonic functions $d_{lmp}$ and their Fourier transforms have been described in *International Tables for Crystallography*, Volume B, Chapter 1.2 (Coppens, 1992). They differ from the functions $y_{lmp}$ by the normalization condition, defined as $\int |d_{lmp}| \, \mathrm{d}\Omega = 2 - \delta_{l0}$. The real spherical harmonic functions are often referred to as *multipoles*, since each

represents the component of the charge distribution $\rho(\mathbf{r})$ that gives a non-zero contribution to the integral for the electrostatic multipole moment $q_{lmp}$,

$$q_{lmp} = -\int \rho_{\rm atom}(\mathbf{r}) r^l c_{lmp}\, \mathrm{d}\mathbf{r}, \qquad (8.7.3.8)$$

where the functions $c_{lmp}$ are the Cartesian representations of the real spherical harmonics (Coppens, 1992).

More general models include non-atom centred functions. If the wavefunction $\psi$ in (8.7.2.4) is an antisymmetrized product of molecular orbitals $\psi_i$, expressed in terms of a linear combination of atomic orbitals $\chi_\mu$, $\psi_i = \sum_\mu c_{i\mu}\chi_\mu$ (LCAO formalism), the integration (8.7.2.4) leads to

$$\rho(\mathbf{r}) = \sum_\mu \sum_\nu P_{\mu\nu}\chi_\mu(\mathbf{r}-\mathbf{R}_\mu)\chi_\nu(\mathbf{r}-\mathbf{R}_\nu), \qquad (8.7.3.9)$$

with $\mathbf{R}_\mu$ and $\mathbf{R}_\nu$ defining the centres of $\chi_\mu$ and $\chi_\nu$, respectively, $P_{\mu\nu} = \sum_i n_i c_{i\mu} c_{i\nu}$, and the sum is over all molecular orbitals with occupancy $n_i$. Expression (8.7.3.9) contains products of atomic orbitals, which may have significant values for orbitals centred on adjacent atoms. In the 'charge-cloud' model (Hellner, 1977), these products are approximated by bond-centred, Gaussian-shaped density functions. Such functions can often be projected efficiently into the one-centre terms of the spherical harmonic multipole model, so that large correlations occur if both spherical harmonics and bond-centred functions are adjusted independently in a least-squares refinement.

According to (8.7.2.4) and (8.7.3.9), the population of the two-centre terms is related to the one-centre occupancies. A molecular-orbital based model, which implicitly incorporates such relations, has been used to describe local bonding between transition-metal and ligand atoms (Becker & Coppens, 1985).

### 8.7.3.3. *Physical constraints*

There are several physical constraints that an electron-density model must satisfy. With the exception of the electroneutrality constraint, they depend strongly on the electron density close to the nucleus, which is poorly determined by the diffraction experiment.

#### 8.7.3.3.1. *Electroneutrality constraint*

Since a crystal is neutral, the total electron population must equal the sum of the nuclear charges of the constituent atoms. A constraint procedure for linear least squares that does not increase the size of the least-squares matrix has been described by Hamilton (1964). If the starting point is a neutral crystal, the constraint equation becomes

$$\sum \Delta P_i S_i = 0, \qquad (8.7.3.10)$$

where $S_i = \int g(\mathbf{r})\, \mathrm{d}\mathbf{r}$, $g$ being a general density function, and the $\Delta P_i$ are the shifts in the population parameters. For the multipole model, only the monopolar functions integrate to a non-zero value. For normalized monopole functions, this gives

$$\sum_{\rm monopoles} \Delta P_i = 0. \qquad (8.7.3.11)$$

If the shifts without constraints are given by the vector $\mathbf{y}$ and the constrained shifts by $\mathbf{y}_c$, the Hamilton constraint is expressed as

$$\mathbf{y}_c^T = \mathbf{y}^T - \mathbf{y}^T \boldsymbol{Q}^T (\boldsymbol{Q}\boldsymbol{A}^{-1}\boldsymbol{Q}^T)^{-1}\boldsymbol{Q}\boldsymbol{A}^{-1}, \qquad (8.7.3.12)$$

where the superscript $T$ indicates transposition, $\boldsymbol{A}$ is the least-squares matrix of the products of derivatives, and $\boldsymbol{Q}$ is a row vector of the values of $S_i$ for elements representing density functions and zeros otherwise.

Expression (8.7.3.12) cannot be applied if the unconstrained refinement corresponds to a singular matrix. This would be the case if all population parameters, including those of the core functions, were to be refined together with the scale factor. In this case, a new set of independent parameters must be defined, as described in Chapter 8.1 on least-squares refinements. Alternatively, one may set the scale factor to one and rescale the population parameters to neutrality after completion of the refinement. This will in general give a non-integral electron population for the core functions. The proper interpretation of such a result is that a core-like function is an appropriate component of the density basis set representing the valence electrons.

#### 8.7.3.3.2. *Cusp constraint*

The electron density at a nucleus $i$ with nuclear charge $Z_i$ must satisfy the electron–nuclear cusp condition given by

$$\lim_{\mathbf{r}_i \to 0} \left( \frac{\partial}{\partial \mathbf{r}_i} + 2Z_i \right) \rho_{0i}(\mathbf{r}_i) = 0, \qquad (8.7.3.13)$$

where $\rho_{0i}(\mathbf{r}_i) = (1/4\pi)\int \rho(\mathbf{r})\, \mathrm{d}\Omega_i$ is the spherical component of the expansion of the density around nucleus $i$.

Only 1$s$-type functions have non-zero electron density at the nucleus and contribute to (8.7.3.13). For the hydrogen-like atom or ion described by a single exponent radial function $R(r) = N\exp(-\zeta r)$, (8.7.3.13) gives $\zeta = 2Z/a_0$, where $Z$ is the nuclear charge, and $a_0$ is the Bohr unit. Thus, a modification of $\zeta$ for 1$s$ functions, as implied by (8.7.3.6) and (8.7.3.7) if applied to H atoms, leads to a violation of the cusp constraint. In practice, the electron density at the nucleus is not determined by a limited resolution diffraction experiment; the single exponent function $R(r)$ is fitted to the electron density away from, rather than at the nucleus.

#### 8.7.3.3.3. *Radial constraint*

Poisson's electrostatic equation gives a relation between the gradient of the electric field $\nabla^2\Phi(\mathbf{r})$ and the electron density at $\mathbf{r}$.

$$\nabla^2\Phi(\mathbf{r}) = -4\pi\rho(\mathbf{r}). \qquad (8.7.3.14)$$

As noted by Stewart (1977), this equation imposes a constraint on the radial functions $R(r)$. For $R_l(r) = N_l r^{n(l)}\exp(-\zeta_l r)$, the condition $n(l) \geq l$ must be obeyed for $R_l r^{-l}$ to be finite at $r = 0$, which satisfies the requirement of the non-divergence of the electric field $\nabla V$, its gradient $\nabla^2 V$, the gradient of the field gradient $\nabla^3 V$, *etc.*

#### 8.7.3.3.4. *Hellmann–Feynman constraint*

According to the electrostatic Hellmann–Feynman theorem, which follows from the Born–Oppenheimer approximation and the condition that the forces on the nuclei must vanish when the nuclear configuration is in equilibrium, the nuclear repulsions are balanced by the electron–nucleus attractions (Levine, 1983). The balance of forces is often achieved by a very sharp polarization of the electron density very close to the nuclei (Hirshfeld & Rzotkiewicz, 1974), which may be represented in the X-ray model by the introduction of dipolar functions with large values of $\zeta$. The Hellmann–Feynman constraint offers the possibility for obtaining information on such functions even though they may contribute only marginally to the observed X-ray scattering (Hirshfeld, 1984).

As the Hellmann–Feynman constraint applies to the static density, its application presumes a proper deconvolution of the thermal motion and the electron density in the scattering model.

8.7.3.4. *Electrostatic moments and the potential due to a charge distribution*

8.7.3.4.1. *Moments of a charge distribution**

Use of the expectation value expression

$$\langle O\rangle = \int \widehat{O}\rho(\mathbf{r})\,\mathrm{d}\mathbf{r}, \tag{8.7.3.15}$$

with the operator $\widehat{O} = \widehat{\gamma} r_{\alpha_1} r_{\alpha_2} r_{\alpha_3} \ldots r_{\alpha_l} = r_{\alpha_1} r_{\alpha_2} r_{\alpha_3} \ldots r_{\alpha_l}$ gives for the electrostatic moments of a charge distribution $\rho(\mathbf{r})$

$$\mu_{\alpha_1\alpha_2\alpha_3\ldots\alpha_l} = \int \rho(\mathbf{r}) r_{\alpha_1} r_{\alpha_2} r_{\alpha_3} \ldots r_{\alpha_l}\,\mathrm{d}\mathbf{r}, \tag{8.7.3.16}$$

in which the $r_\alpha$ are the three components of the vector $\mathbf{r}$ ($\alpha_i = 1, 2, 3$), and the integral is over the complete volume of the distribution.

For $l = 0$, (8.7.3.16) represents the integral over the charge distribution, which is the total charge, a scalar function described as the *monopole*. The higher moments are, in ascending order of $l$, the *dipole*, a vector, the *quadrupole*, a second-rank tensor, and the *octupole*, a third-rank tensor. Successively higher moments are named the *hexadecapole* ($l = 4$), the *tricontadipole* ($l = 5$), and the *hexacontatetrapole* ($l = 6$). An alternative, traceless, definition is often used for moments with $l \geq 2$. In the traceless definition, the quadrupole moment, $\Theta_{\alpha\beta}$, is given by

$$\Theta_{\alpha\beta} = \tfrac{1}{2}\int \rho(\mathbf{r})\left[3r_\alpha r_\beta - r^2\delta_{\alpha\beta}\right]\mathrm{d}r, \tag{8.7.3.17}$$

where $\delta_{\alpha\beta}$ is the Kronecker delta function. The term $\int \rho(\mathbf{r}) r^2\,\mathrm{d}r$, which is subtracted from the diagonal elements of the tensor, corresponds to the spherically averaged second moment of the distribution.

Expression (8.7.3.17) is a special case of the following general expression for the $l$th-rank traceless tensor elements.

$$M^{(l)}_{\alpha_1\alpha_2\ldots\alpha_l} = \frac{(-1)^l}{l!}\int \rho(\mathbf{r}) r^{2l+1} \frac{\partial^l}{\partial r_{\alpha_1}\partial r_{\alpha_2}\ldots\partial r_{\alpha_l}}\left(\frac{1}{r}\right)\mathrm{d}\mathbf{r}. \tag{8.7.3.18}$$

Though the traceless moments can be derived from the unabridged moments, the converse is not the case because the information on the spherically averaged moments is no longer present in the traceless moments. The general relations between the traceless moments and the unabridged moments follow from (8.7.3.18). For the quadrupole moments, we obtain with (8.7.3.17)

$$\begin{aligned}\Theta_{xx} &= \tfrac{3}{2}\mu_{xx} - \tfrac{1}{2}\left(\mu_{xx} + \mu_{yy} + \mu_{zz}\right)\\ &= \mu_{xx} - \tfrac{1}{2}\left(\mu_{yy} + \mu_{zz}\right),\end{aligned}$$

and

$$\Theta_{xy} = \tfrac{3}{2}\mu_{xy}. \tag{8.7.3.19}$$

Expressions for the other elements are obtained by simple permutation of the indices.

For a site of point symmetry 1, the electrostatic moment $\mu_{\alpha_1\alpha_2\alpha_3\ldots\alpha_l}$ of order $l$ has $(l+1)(l+2)/2$ unique elements. In the traceless definition, not all elements are independent. Because the trace of the tensor has been set to zero, only $2l+1$ *independent* components remain. For the quadrupole there are 5 *independent* components of the form (8.7.3.19).

In a different form, the traceless moment operators can be written as the Cartesian spherical harmonics $c_{lmp}$ (*IT*B, 1992) multiplied by $r^l$, which defines the *spherical* electrostatic moments

$$\Theta_{lmp} = \int \rho(\mathbf{r}) c_{lmp} r^l\,\mathrm{d}r. \tag{8.7.3.20}$$

The expressions for $c_{lmp}$ are listed in Volume B of *International Tables for Crystallography* (*IT*B, 1992); for the $l = 2$ moment, the $c_{lmp}$ have the well known form $3z^2 - 1$, $xz$, $yz$, $(x^2 - y^2)/2$, and $xy$, where $x$, $y$ and $z$ are the components of a unit vector from the origin to the point being described. The spherical electrostatic moments have $(2l+1)$ components, which equals the number of independent components in the traceless definition (8.7.3.18), as it should. The linear relationships are

$$\begin{aligned}\Theta_{zz} &= (1/2)\Theta_{20},\\ \Theta_{xx} &= (1/2)\left[3\Theta_{22+} - (1/2)\Theta_{20}\right],\\ \Theta_{yy} &= (1/2)\left[-3\Theta_{22+} - (1/2)\Theta_{20}\right],\\ \Theta_{xz} &= (3/2)\Theta_{21+},\\ \Theta_{yz} &= (3/2)\Theta_{21-},\\ \Theta_{xy} &= (3/2)\Theta_{22-}.\end{aligned} \tag{8.7.3.21}$$

8.7.3.4.1.1. *Moments as a function of the atomic multipole expansion*

In the multipole model [expression (8.7.3.7)], the charge density is a sum of atom-centred density functions, and the moments of a whole distribution can be written as a sum over the atomic moments plus a contribution due to the shift to a common origin. An atomic moment is obtained by integration over the charge distributions $\rho_{\mathrm{total},i}(\mathbf{r}) = \rho_{\mathrm{nuclear},i} - \rho_{e,i}$ of atom $i$,

$$\mu_{\alpha_1\alpha_2\alpha_3\ldots\alpha_l} = \int \rho_{\mathrm{total},i}(\mathbf{r}) r_{\alpha_1} r_{\alpha_2} r_{\alpha_3} \ldots r_{\alpha_l}\,\mathrm{d}r, \tag{8.7.3.22}$$

where the electronic part of the atomic charge distribution is defined by the multipole expansion

$$\begin{aligned}\rho_{e,i}(\mathbf{r}) = {} & P_{i,c}\rho_{\mathrm{core}}(r) + P_{i,v}\kappa_i^3\rho_{i,\mathrm{valence}}(\kappa_i r)\\ & + \sum_{l=0}^{l_{\max}} \kappa_i'^3 R_{i,l}\left(\kappa_i' r\right)\sum_{m=0}^{l}\sum_{p} P_{i,lmp} d_{lmp}(\theta,\varphi),\end{aligned} \tag{8.7.3.23}$$

where $p = \pm$ when $m > 0$, and $R_l(\kappa_i' r)$ is a radial function.

We get for the $j$th moment of the valence density

$$\begin{aligned}\mu^j &= \mu_{\alpha_1\alpha_2\alpha_3\ldots\alpha_j}\\ &= -\int\left[P_{i,v}\kappa_i^3\rho_{i,\mathrm{valence}}(\kappa_i r) + \sum_{l=0}^{l_{\max}}\kappa_i'^3 R_{i,l}\left(\kappa_i' r\right)\right.\\ &\quad\left.\times\sum_{m=0}^{l}\sum_{p} P_{i,lmp} d_{lmp}(\theta,\varphi)\right] r_{\alpha_1} r_{\alpha_2}\ldots r_{\alpha_j}\,\mathrm{d}\mathbf{r},\end{aligned} \tag{8.7.3.24}$$

in which the minus sign arises because of the negative charge of the electrons.

We will use the symbol $\widehat{O}$ for the moment operators. We get

$$\mu^j = -\kappa_i'^3\int \widehat{O}_j \sum_{l=1}^{l_{\max}}\left[\sum_{m=0}^{l}\sum_{p} P_{lmp} d_{lmp} R_l\right]\mathrm{d}\mathbf{r}, \tag{8.7.3.25}$$

where, as before, $p = \pm$. The requirement that the integrand be totally symmetric means that only the dipolar terms in the multipole expansion contribute to the dipole moment. If we use the traceless definition of the higher moments, or the equivalent definition of the moments in terms of the spherical harmonic functions, only the quadupolar terms of the multipole expansion will contribute to the quadrupole moment; more generally, in the traceless definition *the lth-order multipoles are the sole contributors to the lth moments*. In terms of the spherical moments, we get

* An excellent review of experimental results has appeared in the literature (Spackman, 1992).

$$\Theta_{lmp} = -P_{lmp} \int \widehat{O}_{lmp} \left[ d_{lmp} R_l \right] \mathrm{d}\mathbf{r}. \tag{8.7.3.26}$$

Substitution with $R_l = \{(\kappa'\zeta)^{n(l)+3}/[n(l)+2]!\} r^{n(l)} \exp(-\zeta r)$ and $\widehat{O}_{lmp} = c_{lmp} r^l$ and subsequent integration over $r$ gives

$$\Theta_{lmp} = -P_{lmp} \frac{1}{(\kappa'\zeta)^l} \frac{[n(l)+l+2]!}{[n(l)+2]!} \frac{1}{D_{lm} M_{lm}} \int y_{lmp}^2 \sin\theta \, \mathrm{d}\theta \, \mathrm{d}\varphi, \tag{8.7.3.27}$$

where the definitions

$$d_{lmp} = L_{lm} c_{lmp} = \left( \frac{L_{lm}}{M_{lm}} \right) y_{lmp} \quad \text{and} \quad c_{lmp} = \left( \frac{1}{M_{lm}} \right) y_{lmp} \tag{8.7.3.28}$$

have been used (*IT*B, 1992). Since the $y_{lmp}$ functions are wavefunction normalized, we obtain

$$\Theta_{lmp} = -P_{lmp} \frac{1}{(\kappa'\zeta)^l} \frac{[n(l)+l+2]!}{[n(l)+2]!} \frac{L_{lm}}{(M_{lm})^2}. \tag{8.7.3.29}$$

Application to dipolar terms with $n(l) = 2$, $L_{lm} = 1/\pi$ and $M_{lm} = (3/4\pi)^{1/2}$ gives the $x$ component of the atomic dipole moment as

$$\mu_x = -\int P_{11+} d_{11+} R_1 x \, \mathrm{d}\mathbf{r} = -\frac{20}{3\kappa'\zeta} P_{11+}. \tag{8.7.3.30}$$

For the atomic quadrupole moments in the spherical definition, we obtain directly, using $n(l) = 2$, $l = 2$ in (8.7.3.29),

$$\Theta_{20} = -\frac{30}{(\kappa'\zeta)^2} \frac{L_{20}}{(M_{20})^2} P_{20} = -\frac{36\sqrt{3}}{(\kappa'\zeta)^2} P_{20}, \tag{8.7.3.31}$$

and, for the other elements,

$$\Theta_{2mp} = -\frac{30}{(\kappa'\zeta)^2} \frac{L_{2m}}{(M_{2m})^2} P_{2mp} = -\frac{6\pi}{(\kappa'\zeta)^2} P_{2mp}. \tag{8.7.3.32}$$

As the traceless quadrupole moments are linear combinations of the spherical quadrupole moments, the corresponding expressions follow directly from (8.7.3.31), (8.7.3.32) and (8.7.3.21). We obtain with $n(2) = 2$

$$\begin{aligned} \Theta_{zz} &= -\frac{18\sqrt{3}}{(\kappa'\zeta)^2} P_{20}, \\ \Theta_{yy} &= +\frac{9}{(\kappa'\zeta)^2} \left( \sqrt{3} P_{20} + \pi P_{22+} \right), \\ \Theta_{xx} &= \frac{9}{(\kappa'\zeta)^2} \left( \sqrt{3} P_{20} - \pi P_{22+} \right), \end{aligned}$$

and

$$\Theta_{xz} = -\frac{9\pi}{(\kappa'\zeta)^2} P_{21+}, \tag{8.7.3.33}$$

and analogously for the other off-diagonal elements.

8.7.3.4.1.2. *Molecular moments based on the deformation density*

The moments derived from the total density $\rho(\mathbf{r})$ and from the deformation density $\Delta\rho(\mathbf{r})$ are not identical. To illustrate the relation for the diagonal elements of the second-moment tensor, we rewrite the $xx$ element as

$$\begin{aligned} \mu_{xx}(\rho_{\text{total}}) &= \int \rho x^2 \, \mathrm{d}\mathbf{r} \\ &= \int \rho_{\text{promolecule}} x^2 \, \mathrm{d}\mathbf{r} + \int \Delta\rho x^2 \, \mathrm{d}\mathbf{r}. \end{aligned} \tag{8.7.3.34}$$

The promolecule is the sum over spherical atom densities, or

$$\begin{aligned} \int \rho_{\text{promolecule}} x^2 \, \mathrm{d}\mathbf{r} &= \int \sum_i \rho_{\text{spherical atom},i} x^2 \, \mathrm{d}\mathbf{r} \\ &= \sum_i \int \rho_{\text{spherical atom},i} x^2 \, \mathrm{d}\mathbf{r}. \end{aligned} \tag{8.7.3.35}$$

If $\mathbf{R}_i = (X_i, Y_i, Z_i)$ is the position vector for atom $i$, each single-atom contribution can be rewritten as

$$\begin{aligned} \mu_{i,xx,\text{spherical atom}} &= \int \rho_{i,\text{spherical atom}} x^2 \, \mathrm{d}\mathbf{r} \\ &= \int \rho_{i,\text{spherical atom}} (x - X_i)^2 \, \mathrm{d}\mathbf{r} \\ &\quad + X_i \int \rho_{i,\text{spherical atom}} 2(x - X_i) \, \mathrm{d}\mathbf{r} \\ &\quad + X_i^2 \int \rho_{i,\text{spherical atom}} \, \mathrm{d}\mathbf{r}. \end{aligned} \tag{8.7.3.36}$$

Since the last two integrals are proportional to the atomic dipole moment and its net charge, respectively, they will be zero for neutral spherical atoms. Substitution in (8.7.3.35) gives, with $\langle (x - X)_i^2 \rangle = \frac{1}{3} \langle r_i^2 \rangle$, and $\langle r_i^2 \rangle = \int \rho_i(r) r^2 \, \mathrm{d}\mathbf{r}$,

$$\int \rho_{\text{promolecule}} x^2 \, \mathrm{d}\mathbf{r} = \tfrac{1}{3} \sum_{\text{atoms}} \langle r^2 \rangle_{\text{spherical atom}}, \tag{8.7.3.37}$$

and, by substitution in (8.7.3.34),

$$\mu_{xx}(\rho_{\text{tot}}) = \mu_{xx}(\Delta\rho) + \tfrac{1}{3} \sum_{\text{atoms}} \langle r^2 \rangle_{\text{spherical atom}}, \tag{8.7.3.38a}$$

with

$$\mu_{xx}(\Delta\rho) = \sum_i \left( \int \Delta\rho_i x^2 \, \mathrm{d}\mathbf{r} + 2X_i \mu_i + X_i^2 q_i \right), \tag{8.7.3.38b}$$

in which $\mu_i$ and $q_i$ are the atomic dipole moment and the charge on atom $i$, respectively.

The last term in (8.7.3.38*a*) can be derived rapidly from analytical expressions for the atomic wavefunctions. Results for Hartree–Fock wavefunctions have been tabulated by Boyd (1977). Since the off-diagonal elements of the second-moment tensor vanish for the spherical atom, the second term in (8.7.3.38*a*) disappears, and the off-diagonal elements are identical for the total and deformation densities.

The relation between the second moments $\mu_{\alpha\beta}$ and the traceless moments $\Theta_{\alpha\beta}$ of the deformation density can be illustrated as follows. From (8.7.3.17), we may write

$$\Theta_{\alpha\beta}(\Delta\rho) = \tfrac{3}{2} \mu_{\alpha\beta}(\Delta\rho) - \tfrac{1}{2} \delta_{\alpha\beta} \int \Delta\rho \, r^2 \, \mathrm{d}\mathbf{r}. \tag{8.7.3.39}$$

Only the spherical density terms contribute to the integral on the right. Assuming for the moment that the spherical deformation is represented by the valence-shell distortion (*i.e.* neglect of the second monopole in the aspherical atom expansion), we have, with density functions $\rho$ normalized to 1, for each atom

$$(\Delta\rho)_{\text{spherical}} = \kappa^3 P_{\text{valence}} \rho_{\text{valence}}(\kappa r) - P^0_{\text{valence}} \rho_{\text{valence}}(r) \tag{8.7.3.40}$$

and

$$\begin{aligned} \int \Delta\rho \, r^2 \, \mathrm{d}\mathbf{r} &= \int \sum_i \left[ \kappa_i^3 P_{\text{valence},i} \rho_{\text{valence},i}(\kappa_i r) \right. \\ &\quad \left. - P^0_{\text{valence},i} \rho_{\text{valence},i}(r) \right] r^2 \, \mathrm{d}\mathbf{r} \\ &= \sum_i \left( P_{\text{valence},i}/\kappa_i^2 - P^0_{\text{valence}} \right) \langle r_i^2 \rangle_{\text{spherical valence shell}} \\ &\quad + R_i^2 \left( P_{\text{valence},i} - P^0_{\text{valence},i} \right), \end{aligned} \tag{8.7.3.41}$$

which, on substitution in (8.7.3.39), gives the required relation.

8.7.3.4.1.3. *The effect of an origin shift on the outer moments*

In general, the multipole moments depend on the choice of origin. This can be seen as follows. Substitution of $\mathbf{r}'_\alpha = \mathbf{r}_\alpha - \mathbf{R}_\alpha$ in (8.7.3.16) corresponds to a shift of origin by $\mathbf{R}_\alpha$, or $\mathbf{X}$, $\mathbf{Y}$, $\mathbf{Z}$ in the original coordinate system. In three dimensions, we get, for the first moment, the charge $q$,

$$q' = q, \tag{8.7.3.42}$$

and for the transformed first and second moments

$$\begin{aligned}
&\mu'_x = \mu_x - q\mathbf{X};\ \ \mu'_y = \mu_y - q\mathbf{Y};\ \ \mu'_z = \mu_z - q\mathbf{Z};\\
&\mu'_{\alpha\alpha} = \mu_{\alpha\alpha} - 2\mu_\alpha R_\alpha + qR_\alpha^2;\\
&\mu'_{\alpha\beta} = \mu_{\alpha\beta} - \mu_\alpha R_\beta - \mu_\beta R_\alpha + qR_\alpha R_\beta.
\end{aligned} \tag{8.7.3.43}$$

For the traceless quadrupole moments, the corresponding equations are obtained by substitution of $\mathbf{r}'_\alpha = \mathbf{r}_\alpha - \mathbf{R}_\alpha$ and $\mathbf{r}' = \mathbf{r} - \mathbf{R}$ into (8.7.3.17), which gives

$$\begin{aligned}
\Theta'_{\alpha\beta} = \Theta_{\alpha\beta} &+ \tfrac{1}{2}\left(3\mathbf{R}_\alpha\mathbf{R}_\beta - \mathbf{R}^2\delta_{\alpha\beta}\right)q\\
&- \tfrac{3}{2}\left(\mathbf{R}_\beta\mu_\alpha + \mathbf{R}_\alpha\mu_\beta\right) + \sum_\gamma\left(\mathbf{R}_\gamma\mu_\gamma\right)\delta_{\alpha\beta}.
\end{aligned} \tag{8.7.3.44}$$

Similar expressions for the higher moments are reported in the literature (Buckingham, 1970).

We note that *the first non-vanishing moment is origin-independent*. Thus, the dipole moment of a neutral molecule, but not that of an ion, is independent of origin; the quadrupole moment of a molecule without charge and dipole moment is not dependent on the choice of origin and so on. The molecular electric moments are commonly reported with respect to the centre of mass.

#### 8.7.3.4.1.4. *Total moments as a sum over the pseudoatom moments*

The moments of a molecule or of a molecular fragment are obtained from the sum over the atomic moments, plus a contribution due to the shift to a common origin for all but the monopoles. If individual atomic coordinate systems are used, as is common if chemical constraints are applied in the least-squares refinement, they must be rotated to have a common orientation. Expressions for coordinate system rotations have been given by Cromer, Larson & Stewart (1976) and by Su & Coppens (1994*a*).

The transformation to a common coordinate origin requires use of the origin-shift expressions (8.7.3.42)–(8.7.3.44), with, for an atom at $\mathbf{r}_i$, $\mathbf{R} = -\mathbf{r}_i$. The first three moments summed over the atoms $i$ located at $\mathbf{r}_i$ become

$$q_{\text{total}} = \sum q_i, \tag{8.7.3.45}$$

$$\mu_{\text{total}} = \sum_i \mu_i + \sum \mathbf{r}_i q_i, \tag{8.7.3.46}$$

and

$$\mu_{\alpha\beta,\text{total}} = \sum_i\left(\mu_{\alpha\beta i} + r'_{\beta i}\mu_\alpha + r'_{\alpha i}\mu_\beta + r'_{\alpha i}r'_{\beta i}q_i\right) \tag{8.7.3.47}$$

with $\alpha, \beta = x, y, z$; and expressions equivalent to (8.7.3.44) for the traceless components $\Theta_{\alpha\beta}$.

#### 8.7.3.4.1.5. *Electrostatic moments of a subvolume of space by Fourier summation*

Expression (8.7.3.16) for the outer moment of a distribution within a volume element $V_T$ may be written as

$$\mu_{\alpha_1\alpha_2\ldots\alpha_l} = \int_{V_T} \rho(\mathbf{r})\widehat{\gamma}_{\alpha_1\alpha_2\alpha_3\ldots\alpha_l}\,\mathrm{d}\mathbf{r}, \tag{8.7.3.16}$$

with $\widehat{\gamma}_{\alpha_1\alpha_2\alpha_3\ldots\alpha_l} = r_{\alpha_1}r_{\alpha_2}r_{\alpha_3}\ldots r_{\alpha_l}$, and integration over the volume $V_T$.

Replacement of $\rho(\mathbf{r})$ by the Fourier summation over the structure factors gives

$$\begin{aligned}
\mu^l_{(V_T)} &= \frac{1}{V}\int_{V_T}\widehat{\gamma}_l\sum F(\mathbf{h})\exp(-2\pi i\mathbf{h}\cdot\mathbf{r})\,\mathrm{d}\mathbf{r}\\
&= \frac{1}{V}\sum F(\mathbf{h})\int_{V_T}\widehat{\gamma}_l\exp(-2\pi i\mathbf{h}\cdot\mathbf{r})\,\mathrm{d}\mathbf{r},
\end{aligned} \tag{8.7.3.48}$$

where $\widehat{\gamma}_l$ is the product of $l$ coordinates according to (8.7.3.16), and $\mu^l$ represents the moment of the static distribution if the $F(\mathbf{h})$ are the structure factors on an absolute scale after deconvolution of thermal motion. Otherwise, the moment of the thermally averaged density is obtained.

The integral $\int_{V_T}\widehat{\gamma}_l\exp(-2\pi i\mathbf{h}\cdot\mathbf{r})\,\mathrm{d}\mathbf{r}$ is defined as the *shape transform* $S$ of the volume $V_T$.

$$\mu^l(V_T) = \frac{1}{V}\sum F(\mathbf{h})S_{V_T}(\widehat{\gamma}_l, \mathbf{h}).$$

For regularly shaped volumes, the integral can be evaluated analytically. A volume of complex shape may be subdivided into integrable subvolumes such as parallelepipeds. By choosing the subvolumes sufficiently small, a desired boundary surface can be closely approximated.

If the origin of each subvolume is located at $\mathbf{r}_i$, relative to a coordinate system origin at $P$, the total electronic moment relative to this origin is given by

$$\mu^l\left(\sum_i V_{T,i}\right) = \frac{1}{V}\sum_{\mathbf{h}} F(\mathbf{h})S_{V_T}(\widehat{\gamma}_l, \mathbf{h})\sum_i \exp(-2\pi i\mathbf{h}\cdot\mathbf{r}_i). \tag{8.7.3.49}$$

Expressions for $S_{V_T}$ for $l \leq 2$ and a subvolume parallelepipedal shape are given in Table 8.7.3.2. Since the spherical order Bessel functions $j_n(x)$ that appear in the expressions generally decrease with increasing $x$, the moments are strongly dependent on the low-order reflections in a data set. An example is the shape transform for the dipole moment. Relative to an origin $O$,

$$S(\widehat{\gamma}_1, \mathbf{h}) = \int_{V_t}\mathbf{r}_0\exp(-2\pi i\mathbf{h}\cdot\mathbf{r}_0)\,\mathrm{d}\mathbf{r}.$$

A shift of origin by $-\mathbf{r}_i$ leads to

$$\begin{aligned}
\mu^{1'}(V_T) &= \frac{1}{V}\sum F(\mathbf{h})\left[S_{V_T}(\widehat{\gamma}_1, \mathbf{h}) + \mathbf{r}_1\int\exp(-2\pi i\mathbf{h}\cdot r_0)\,\mathrm{d}\mathbf{r}\right]\\
&\quad\times\exp(-2\pi i\mathbf{h}\cdot\mathbf{r}_1)\\
&= \mu^1(V_T) + \mathbf{r}_1 q,
\end{aligned}$$

in agreement with (8.7.3.46).

### 8.7.3.4.2. *The electrostatic potential*

#### 8.7.3.4.2.1. *The electrostatic potential and its derivatives*

The electrostatic potential $\Phi(\mathbf{r}')$ due to the electronic charge distribution is given by the Coulomb equation,

$$\Phi(\mathbf{r}') = -k\int\frac{\rho(\mathbf{r})}{|\mathbf{r} - \mathbf{r}'|}\,\mathrm{d}\mathbf{r}, \tag{8.7.3.50}$$

where the constant $k$ is dependent on the units selected, and will here be taken equal to 1. For an assembly of positive point nuclei and a continuous distribution of negative electronic charge, we obtain

$$\Phi(\mathbf{r}') = \sum_M\frac{Z_M}{|\mathbf{R}_M - \mathbf{r}'|} - \int\frac{\rho(\mathbf{r})}{|\mathbf{r} - \mathbf{r}'|}\,\mathrm{d}\mathbf{r}, \tag{8.7.3.51}$$

in which $Z_M$ is the charge of nucleus $M$ located at $\mathbf{R}_M$.

The *electric field* **E** at a point in space is the gradient of the electrostatic potential at that point.

$$\mathbf{E}(\mathbf{r}) = -\nabla\Phi(\mathbf{r}) = -\mathbf{i}\frac{\partial\Phi(\mathbf{r})}{\partial x} - \mathbf{j}\frac{\partial\Phi(\mathbf{r})}{\partial y} - \mathbf{k}\frac{\partial\Phi(\mathbf{r})}{\partial z}. \quad (8.7.3.52)$$

As **E** is the negative gradient vector of the potential, the electric force is directed 'downhill' and proportional to the slope of the potential function. The explicit expression for **E** is obtained by differentiation of the operator $|\mathbf{r}-\mathbf{r}'|^{-1}$ in (8.7.3.50) towards $x, y, z$ and subsequent addition of the vector components. For the negative slope of the potential in the $x$ direction, one obtains

$$\mathbf{E}_x(\mathbf{r}') = \int \frac{\rho_{\rm total}(\mathbf{r})}{|\mathbf{r}'-\mathbf{r}|^2}\,\frac{(\mathbf{r}'-\mathbf{r})_x}{|\mathbf{r}'-\mathbf{r}|}\,{\rm d}\mathbf{r} = \int \frac{\rho_{\rm total}(\mathbf{r})}{|\mathbf{r}'-\mathbf{r}|^3}(\mathbf{r}'-\mathbf{r})_x\,{\rm d}\mathbf{r}, \quad (8.7.3.53)$$

which gives, after addition of the components,

$$\mathbf{E}(\mathbf{r}') = -\nabla\Phi(\mathbf{r}') = \int \frac{\rho_t(\mathbf{r})(\mathbf{r}'-\mathbf{r})}{|\mathbf{r}-\mathbf{r}'|^3}\,{\rm d}\mathbf{r}. \quad (8.7.3.54)$$

The electric field gradient (EFG) is the tensor product of the gradient operator $\nabla = \mathbf{i}\frac{\partial}{\partial x} + \mathbf{j}\frac{\partial}{\partial y} + \mathbf{k}\frac{\partial}{\partial z}$ and the electric field vector **E**;

$$\nabla\mathbf{E} = \nabla : \mathbf{E} = -\nabla : \nabla\Phi. \quad (8.7.3.55)$$

It follows that in a Cartesian system the EFG tensor is a symmetric tensor with elements

$$\nabla\mathbf{E}_{\alpha\beta} = -\frac{\partial^2\Phi}{\partial r_\alpha \partial r_\beta}. \quad (8.7.3.56)$$

The EFG tensor elements can be obtained by differentiation of the operator in (8.7.3.53) for $\mathbf{E}_\alpha$ to each of the three directions $\beta$. In this way, the traceless result

$$\begin{aligned}\nabla\mathbf{E}_{\alpha\beta}(\mathbf{r}') &= \frac{\partial\mathbf{E}_\alpha}{\partial(r_\beta - r'_\beta)} \\ &= -\int \frac{1}{|\mathbf{r}-\mathbf{r}'|^5}\Big\{3(r_\alpha - r'_\alpha)(r_\beta - r'_\beta) \\ &\quad - |\mathbf{r}-\mathbf{r}'|^2\delta_{\alpha\beta}\Big\}\rho_{\rm total}(\mathbf{r})\,{\rm d}\mathbf{r} \end{aligned} \quad (8.7.3.57)$$

is obtained. We note that according to (8.7.3.57) the electric field gradient can equally well be interpreted as the tensor of the traceless quadrupole moments of the distribution $-2\rho_{\rm total}(\mathbf{r})/|\mathbf{r}-\mathbf{r}'|^5$ [see equation (8.7.3.17)].

Definition (8.7.3.56) and result (8.7.3.57) differ in that (8.7.3.56) does not correspond to a zero-trace tensor. The situation is analogous to the two definitions of the second moments, discussed above, and is illustrated as follows. The trace of the tensor defined by (8.7.3.56) is given by

$$-\nabla^2\Phi = -\nabla\cdot\nabla\Phi = -\left(\frac{\partial^2\Phi}{\partial x^2} + \frac{\partial^2\Phi}{\partial y^2} + \frac{\partial^2\Phi}{\partial z^2}\right). \quad (8.7.3.58)$$

Poisson's equation relates the divergence of the gradient of the potential $\Phi(\mathbf{r})$ to the electron density at that point:

$$\nabla^2\Phi(\mathbf{r}) = -4\pi\big[-\rho_e(\mathbf{r})\big] = 4\pi\rho_e(\mathbf{r}). \quad (8.7.3.59)$$

Thus, the EFG as defined by (8.7.3.56) is not traceless, unless the electron density at **r** is zero.

The potential and its derivatives are sometimes referred to as *inner moments* of the charge distribution, since the operators in (8.7.3.50), (8.7.3.52) and (8.7.3.54) contain the negative power of the position vector. In the same terminology, the electrostatic moments discussed in §8.7.3.4.1 are described as the *outer* moments.

Table 8.7.3.2. *Expressions for the shape factors S for a parallelepiped with edges $\delta_x$, $\delta_y$, and $\delta_z$ (from Moss & Coppens, 1981)*

$j_0$ and $j_1$ are the zero- and first-order spherical Bessel functions: $j_0(x) = \sin x/x$, $j_1(x) = \sin x/x^2 - \cos x/x$; $V_T$ is volume of integration.

| $\hat{y}$ | Property | $S[\hat{y}(\mathbf{r}), \mathbf{h}]$ |
|---|---|---|
| 1 | Charge | $V_T j_0(2\pi h_x\delta_x) j_0(2\pi h_y\delta_y) j_0(2\pi h_z\delta_z)$ |
| $r_\alpha$ | Dipole $\mu_\alpha$ | $-iV_T\delta_\alpha j_1(2\pi h_\alpha\delta_\alpha)$ $\times j_0(2\pi h_\beta\delta_\beta) j_0(2\pi h_\gamma\delta_\gamma)$ |
| $r_\alpha r_\beta$ | Second moment $\mu_{\alpha\beta}$ off-diagonal | $-V_T\delta_\alpha\delta_\beta j_1(2\pi h_\alpha\delta_\alpha)$ $\times j_1(2\pi h_\beta\delta_\beta) j_0(2\pi h_\gamma\delta_\gamma)$ |
| $r_\alpha r_\alpha$ | Second moment $\mu_{\alpha\alpha}$ diagonal | $-V_T\delta_\alpha^2\left\{\frac{j_1(2\pi h_\alpha\delta_\alpha)}{\pi h_\alpha\delta_\alpha} - j_0(2\pi h_\alpha\delta_\alpha)\right\}$ $\times j_0(2\pi h_\beta\delta_\beta) j_0(2\pi h_\gamma\delta_\gamma)$ |

It is of interest to evaluate the electric field gradient at the atomic nuclei, which for several types of nuclei can be measured accurately by nuclear quadrupole resonance and Mössbauer spectroscopy. The contribution of the atomic valence shell centred on the nucleus can be obtained by substitution of the multipolar expansion (8.7.3.7) in (8.7.3.57). The quadrupolar ($l = 2$) terms in the expansion contribute to the integral. For the radial function $R_l = \{\zeta^{n(l)+3}/[n(l)+2]!\}r^{n(l)}\exp(-\zeta r)$ with $n(l) = 2$, the following expressions are obtained:

$$\begin{aligned}\nabla\mathbf{E}_{11} &= +(3/5)\Big(\pi P_{22+} - \sqrt{3}P_{20}\Big)Q_r, \\ \nabla\mathbf{E}_{22} &= -(3/5)\Big(\pi P_{22+} + \sqrt{3}P_{20}\Big)Q_r, \\ \nabla\mathbf{E}_{33} &= +(6/5)\Big(\sqrt{3}P_{20}\Big)Q_r, \\ \nabla\mathbf{E}_{12} &= +(3/5)(\pi P_{22-})Q_r, \\ \nabla\mathbf{E}_{13} &= +(3/5)\big(\pi P_{21+}\big)Q_r, \\ \nabla\mathbf{E}_{23} &= +(3/5)(\pi P_{21-})Q_r, \end{aligned} \quad (8.7.3.60)$$

with

$$\begin{aligned} Q_r &= \big\langle r^3\big\rangle_{3\,\rm d} \\ &= \int_0^\infty [R(r)/r]\,{\rm d}r \\ &= (\kappa'\zeta)^3/[n_2(n_2+1)(n_2+2)] \\ &= (\kappa'\zeta)^3/120, \end{aligned}$$

in the case that $n_2 = 4$ (Stevens, DeLucia & Coppens, 1980).

The contributions of neighbouring atoms can be subdivided into point-charge, point-multipole, and penetration terms, as discussed by Epstein & Swanton (1982) and Su & Coppens (1992, 1994*b*), where appropriate expressions are given. Such contributions are in particular important when short interatomic distances are involved. For transition-metal atoms in coordination complexes, the contribution of neighbouring atoms is typically much smaller than the valence contribution.

8.7.3.4.2.2. *Electrostatic potential outside a charge distribution*

Hirshfelder, Curtiss & Bird (1954) and Buckingham (1959) have given an expression for the potential at a point $\mathbf{r}_i$ outside a charge distribution:

$$\Phi(\mathbf{r}_i) = \frac{q}{r_i} + \frac{\mu_\alpha r_\alpha}{r_i^3} + \tfrac{1}{2}\left[3r_\alpha r_\beta - r^2\delta_{\alpha\beta}\right]\frac{\Theta_{\alpha\beta}}{r_i^5} + \left[5r_\alpha r_\beta r\gamma - r^2\left(r_\alpha\delta_{\beta\gamma} + r_\beta\delta_{\gamma\alpha} + r_\gamma\delta_{\alpha\beta}\right)\right]\frac{\Omega_{\alpha\beta\gamma}}{5r_i^7} + \ldots, \tag{8.7.3.61}$$

where summation over repeated indices is implied. The outer moments $q$, $\mu_\alpha$, $\Phi_{\alpha\beta}$ and $\Omega_{\alpha\beta\gamma}$ in (8.7.3.61) must include the nuclear contributions, but, for a point outside the distribution, the spherical neutral-atom densities and the nuclear contributions cancel, so that the potential outside the charge distribution can be calculated from the deformation density.

The summation in (8.7.3.61) is slowly converging if the charge distribution is represented by a single set of moments. When dealing with experimental charge densities, a multicentre expansion is available from the analysis, and (8.7.3.61) can be replaced by a summation over the distributed moments centred at the nuclear positions, in which case $r_i$ measures the distance from a centre of the expansion to the field point. The result is equivalent to more general expressions given by Su & Coppens (1992), which, for very large values of $r_i$, reduce to the sum over atomic terms, each expressed as (8.7.3.61). The interaction between two charge distributions, $A$ and $B$, is given by

$$E_{AB} = \int \Phi_A(\mathbf{r})\rho_B(\mathbf{r})\,\mathrm{d}\mathbf{r},$$

where $\rho_B$ includes the nuclear charge distribution.

8.7.3.4.2.3. *Evaluation of the electrostatic functions in direct space*

The electrostatic properties of a well defined group of atoms can be derived directly from the multipole population coefficients. This method allows the 'lifting' of a molecule out of the crystal, and therefore the examination of the electrostatic quantities at the periphery of the molecule, the region of interest for intermolecular interactions. The difficulty related to the origin term, encountered in the reciprocal-space methods, is absent in the direct-space analysis.

In order to express the functions as a sum over atomic contributions, we rewrite (8.7.3.51), (8.7.3.54) and (8.7.3.57) for the electrostatic properties at point $P$ as a sum over atomic contributions.

$$\Phi(\mathbf{R}_p) = \sum_{M\neq P}\frac{Z_M}{|\mathbf{R}_{MP}|} - \sum_M\int\frac{\rho_{e,M}(\mathbf{r}_M)}{|\mathbf{r}_p|}\,\mathrm{d}\mathbf{r}_M, \tag{8.7.3.62}$$

$$\mathbf{E}(\mathbf{R}_p) = -\sum_{M\neq P}\frac{Z_{MP}\mathbf{R}_{MP}}{|\mathbf{R}_{MP}|^3} + \sum_M\int\frac{\mathbf{r}_p\rho_{e,M}(\mathbf{r}_M)}{|\mathbf{r}_p|^3}\,\mathrm{d}\mathbf{r}_M, \tag{8.7.3.63}$$

$$\nabla\mathbf{E}_{\alpha\beta}(\mathbf{R}_p) = -\sum_{M\neq P}\frac{Z_M(3R_\alpha R_\beta - \delta_{\alpha\beta}|R_{MP}|^2)}{|R_{MP}|^5} + \sum_M\int\frac{\rho_{e,M}(\mathbf{r}_M)(3r_\alpha r_\beta - \delta_{\alpha\beta}|\mathbf{r}_p|^2)}{|\mathbf{r}_p|^5}\,\mathrm{d}\mathbf{r}_M, \tag{8.7.3.64}$$

in which the exclusion of $M = P$ only applies when the point $P$ coincides with a nucleus, and therefore only occurs for the central contributions. $Z_M$ and $\mathbf{R}_M$ are the nuclear charge and the position vector of atom $M$, respectively, while $\mathbf{r}_P$ and $\mathbf{r}_M$ are, respectively, the vectors from $P$ and from the nucleus $M$ to a point $\mathbf{r}$, such that $\mathbf{r}_P = \mathbf{r} - \mathbf{R}_P$, and $\mathbf{r}_M = \mathbf{r} - \mathbf{R}_M = \mathbf{r}_P + \mathbf{R}_P - \mathbf{R}_M = \mathbf{r}_P - \mathbf{R}_{MP}$. The subscript $M$ in the second, electronic part of the expressions refers to density functions centred on atom $M$.

Expressions for the evaluation of (8.7.3.62)–(8.7.3.64) from the charge-density parameters of the multipole expansion have been given by Su & Coppens (1992). They employ the Fourier convolution theorem, used by Epstein & Swanton (1982) to evaluate the electric field gradient at the atomic nuclei. A direct-space method based on the Laplace expansion of $1/|\mathbf{R}_p - \mathbf{r}|$ was reported by Bentley (1981).

8.7.3.4.3. *Electrostatic functions of crystals by modified Fourier summation*

Expression (8.7.3.49) is an example of derivation of electrostatic properties by direct Fourier summations of the structure factors. The electrostatic potential and its derivatives may be obtained in an analogous manner.

In order to obtain the electrostatic properties of the total charge distribution, it is convenient to define the 'total' structure factor $F_{\text{total}}(\mathbf{h})$ including the nuclear contribution,

$$F_{\text{total}}(\mathbf{h}) = F_N(\mathbf{h}) - F(\mathbf{h}),$$

where $F_N(\mathbf{h}) = \sum_j Z_j\exp(2\pi i\mathbf{h}\cdot\mathbf{R}_j)$, the summation being over all atoms $j$ with nuclear charge $Z_j$, located at $R_j$. If $\Phi(\mathbf{h})$ is defined as the Fourier transform of the direct-space potential, we have

$$\Phi(\mathbf{r}) = \int\Phi(\mathbf{h})\exp(-2\pi i\mathbf{h}\cdot\mathbf{r})\,\mathrm{d}\mathbf{h}$$

and

$$\nabla^2\Phi(\mathbf{r}) = -4\pi^2\int h^2\Phi(\mathbf{h})\exp(-2\pi i\mathbf{h}\cdot\mathbf{r})\,\mathrm{d}\mathbf{h},$$

which equals $-4\pi\rho_{\text{total}}$ according to the Poisson equation (8.7.3.59). One obtains with

$$\rho_{\text{total}}(\mathbf{r}) = \int F_{\text{total}}(\mathbf{h})\exp(-2\pi i\mathbf{h}\cdot\mathbf{r})\,\mathrm{d}\mathbf{h},$$
$$\Phi(\mathbf{h}) = +F_{\text{total}}(\mathbf{h})/\pi h^2, \tag{8.7.3.65}$$

and, by inverse Fourier transformation of (8.7.3.65),

$$\Phi(\mathbf{r}) = \frac{1}{\pi V}\sum F_{\text{total}}(\mathbf{h})/h^2\exp(-2\pi i\mathbf{h}\cdot\mathbf{r}) \tag{8.7.3.66}$$

(Bertaut, 1978; Stewart, 1979). Furthermore, the electric field due to the electrons is given by

$$\mathbf{E}(\mathbf{r}) = -\nabla_r\Phi(\mathbf{r}) = -\nabla\int\Phi(\mathbf{h})\exp(-2\pi i\mathbf{h}\cdot\mathbf{r})\,\mathrm{d}\mathbf{h} = 2\pi i\int\mathbf{h}\Phi(\mathbf{h})\exp(-2\pi i\mathbf{h}\cdot\mathbf{r})\,\mathrm{d}\mathbf{h}.$$

Thus, with (8.7.3.65),

$$\mathbf{E}(\mathbf{r}) = \frac{2i}{V}\sum\left[F_{\text{total}}(\mathbf{h})/h^2\right]\mathbf{h}\exp(-2\pi i\mathbf{h}\cdot\mathbf{r}), \tag{8.7.3.67a}$$

which implies

$$\mathbf{E}(\mathbf{h}) = \frac{2i}{h^2}\mathbf{h}F_{\text{total}}(\mathbf{h}).$$

Similarly, the $\mathbf{h}$ Fourier component of the electric field gradient tensor with trace $4\pi\rho(\mathbf{r})$ is

$$[\nabla:\mathbf{E}](\mathbf{h}) = +4\pi^2\mathbf{h}:\mathbf{h}\Phi(\mathbf{h}) = +4\pi\mathbf{h}:\mathbf{h}F_{\text{total}}(\mathbf{h})/h^2, \tag{8.7.3.67b}$$

where $\mathbf{i}:\mathbf{k}$ represents the tensor product of two vectors. This leads to the expression for the electric field gradient in direct space,

$$[\nabla:\mathbf{E}](\mathbf{r}) = \frac{4\pi}{V}\sum \mathbf{h}:\mathbf{h}F_{\text{total}}(\mathbf{h})/h^2 \exp(-2\pi i\mathbf{h}\cdot\mathbf{r}). \quad (8.7.3.68)$$

(The elements of $\mathbf{h}:\mathbf{h}$ are the products $h_ih_j$.)

The components of $\mathbf{E}$ and the elements of the electric field gradient defined by (8.7.3.67*a*) and (8.7.3.68) are with respect to the reciprocal-lattice coordinate system. Proper transforms are required to get the values in other coordinate systems. Furthermore, to get the traceless $\nabla\mathbf{E}$ tensor, the quantity $-(4\pi/3)\rho_e(\mathbf{r}) = -(4\pi/3V)\sum F(\mathbf{h})\exp(-2\pi i\mathbf{h}\cdot\mathbf{r})$ must be subtracted from each of the diagonal elements $\nabla\mathbf{E}_{ii}$.

The Coulombic self-electronic energy of the crystal can be obtained from

$$\begin{aligned} E_{\text{Coulombic, electronic}} &= \tfrac{1}{2}\int\int \frac{\rho_e(\mathbf{r})\rho_e(\mathbf{r}')}{|\mathbf{r}-\mathbf{r}'|}\,\mathrm{d}\mathbf{r}\,\mathrm{d}\mathbf{r}', \\ &= \tfrac{1}{2}\int \Phi_e(\mathbf{r})\rho(\mathbf{r})\,\mathrm{d}\mathbf{r}. \end{aligned}$$

Since $\int \Phi(\mathbf{r})\rho(\mathbf{r})\,\mathrm{d}\mathbf{r} = \int \Phi(\mathbf{h})F(\mathbf{h})\,\mathrm{d}\mathbf{h}$ (Parseval's rule), the summation can be performed in reciprocal space,

$$E_{\text{Coulombic, electronic}} = \frac{1}{2\pi V}\sum F^2(\mathbf{h})/h^2, \quad (8.7.3.69a)$$

and, for the total Coulombic energy,

$$E_{\text{Coulombic, total}} = \frac{1}{2\pi V}\sum F^2_{\text{total}}(\mathbf{h})/h^2, \quad (8.7.3.69b)$$

where the integral has been replaced by a summation.

The summations are rapidly convergent, but suffer from having a singularity at $\mathbf{h}=0$ (Dahl & Avery, 1984; Becker & Coppens, 1990). The contribution from this term to the potential cannot be ignored if different structures are compared. The term at $\mathbf{h}=0$ gives a constant contribution to the potential, which, however, has no effect on the energy of a neutral system. For polar crystals, an additional term occurs in (8.7.3.69*a*, *b*), which is a function of the dipole moment $D$ of the unit cell (Becker, 1990),

$$E_{\text{Coulombic, total}} = \frac{1}{2\pi V}\sum F^2_{\text{total}}(\mathbf{h})/h^2 + \frac{2\pi}{3V}D^2. \quad (8.7.3.69c)$$

To obtain the total energy of the static crystal, electron exchange and correlation as well as electron kinetic energy contributions must be added.

#### 8.7.3.4.4. *The total energy of a crystal as a function of the electron density*

One can write the total energy of a system as

$$E = e_c[\rho] + T + E_{xc}, \quad (8.7.3.70)$$

where $T$ is the kinetic energy, $E_{xc}$ represents the exchange and electron correlation contributions, and $E_c[\rho]$, the Coulomb energy, discussed in the previous section, is given by

$$E_c = \tfrac{1}{2}\sum_{i\neq j}\frac{Z_iZ_j}{R_{ij}} - \sum_i Z_i\Phi(\mathbf{R}_i) + \tfrac{1}{2}\int\int \frac{\rho(\mathbf{r})\rho(\mathbf{r}')}{|\mathbf{r}-\mathbf{r}'|}\,\mathrm{d}\mathbf{r}\,\mathrm{d}\mathbf{r}', \quad (8.7.3.71)$$

where $Z_i$ is the nuclear charge for an atom at position $\mathbf{R}_i$, and $\mathbf{R}_{ij} = \mathbf{R}_j - \mathbf{R}_i$.

Because of the theorem of Hohenberg & Kohn (1964), $E$ is a unique functional of the electron density $\rho$, so that $T + E_{xc}$ must be a functional of $\rho$. Approximate density functionals are discussed extensively in the literature (Dahl & Avery, 1984) and are at the centre of active research in the study of electronic structure of various materials. Given an approximate functional, one can estimate non-Coulombic contributions to the energy from the charge density $\rho(\mathbf{r})$.

In the simplest example, the functionals are those applicable to an electronic gas with slow spatial variations (the 'nearly free electron gas'). In this approximation, the kinetic energy $T$ is given by

$$T = c_k\int \rho t[\rho]\,\mathrm{d}^3\mathbf{r}, \quad (8.7.3.72)$$

with $c_k = (3/10)(2\pi^2)^{2/3}$; and the function $t[\rho] = \rho^{2/3}$. The exchange-correlation energy is also a functional of $\rho$,

$$E_{xc} = -c_x\int \rho e_{xc}[\rho]\,\mathrm{d}^3\mathbf{r},$$

with $c_x = (3/4)(3/\pi)^{1/3}$ and $e_{xc}[\rho] = \rho^{1/3}$.

Any attempt to minimize the energy with respect to $\rho$ in this framework leads to very poor results. However, cohesive energies can be described quite well, assuming that the change in electron density due to cohesive forces is slowly varying in space.

An example is the system $AB$, with closed-shell subsystems $A$ and $B$. Let $\rho_A$ and $\rho_B$ be the densities for individual $A$ and $B$ subsystems. The interaction energy is written as

$$\begin{aligned} \Delta E = {} & E_c[\rho] - E_c[\rho_A] - E_c[\rho_B] \\ & + c_k\int \mathrm{d}\mathbf{r}\{\rho t[\rho] - \rho_A t[\rho_A] - \rho_B t[\rho_B]\} \\ & - c_x\int \mathrm{d}\mathbf{r}\{\rho e_{xc}[\rho] - \rho_A e_{xc}[\rho_A] - \rho_B e_{xc}[\rho_B]\}. \end{aligned} \quad (8.7.3.73)$$

This model is known as the Gordon–Kim (1972) model and leads to a qualitatively valid description of potential energy surfaces between closed-shell subsystems. Unlike pure Coulombic models, this density functional model can lead to an equilibrium geometry. It has the advantage of depending only on the charge density $\rho$.

#### 8.7.3.5. *Quantitative comparison with theory*

Frequently, the purpose of a charge density analysis is comparison with theory at various levels of sophistication. Though the charge density is a detailed function, the features of which can be compared at several points of interest in space, it is by no means the only level at which comparison can be made. The following sequence represents a progression of functions that are increasingly related to the experimental measurement.

$$\begin{array}{lll} & & \text{electrostatic properties} \\ & & \uparrow \\ \psi(1,2,\ldots,n) \rightarrow \Gamma^1(1,1) & \rightarrow \rho(\mathbf{r}) \rightarrow & \langle\rho(\mathbf{r})\rangle \rightarrow F(\mathbf{h}) \rightarrow I(\mathbf{h}) \\ & \downarrow & \\ & \Delta\rho(\mathbf{r}) \rightarrow & \langle\Delta\rho(\mathbf{r})\rangle, \end{array} \quad (8.7.3.74)$$

where the angle brackets refer to the thermally averaged functions.

The experimental information may be reduced in the opposite sequence:

Table 8.7.3.3. *The matrix $M^{-1}$ relating d-orbital occupancies $P_{ij}$ to multipole populations $P_{lm}$ (from Holladay, Leung & Coppens, 1983)*

| $d$-orbital populations | Multipole populations | | | | | |
|---|---|---|---|---|---|---|
| | $P_{00}$ | $P_{20}$ | $P_{22+}$ | $P_{40}$ | $P_{42+}$ | $P_{44+}$ |
| $P_z^2$ | 0.200 | 1.039 | 0.00 | 1.396 | 0.00 | 0.00 |
| $P_{xz}$ | 0.200 | 0.520 | 0.942 | −0.931 | 1.108 | 0.00 |
| $P_{yz}$ | 0.200 | 0.520 | −0.942 | −0.931 | −1.108 | 0.00 |
| $P_{x^2-y^2}$ | 0.200 | −0.039 | 0.00 | 0.233 | 0.00 | 1.571 |
| $P_{xy}$ | 0.200 | −1.039 | 0.00 | 0.233 | 0.00 | −1.571 |

Mixing terms

| | $P_{21}$ | $P_{21-}$ | $P_{22+}$ | $P_{22-}$ | $P_{41+}$ | $P_{41-}$ | $P_{42+}$ | $P_{42-}$ | $P_{43+}$ | $P_{43-}$ | $P_{44-}$ |
|---|---|---|---|---|---|---|---|---|---|---|---|
| $P_{z^2/xz}$ | 1.088 | 0.00 | 0.00 | 0.00 | 2.751 | 0.00 | 0.00 | 0.00 | 0.00 | 0.00 | 0.00 |
| $P_{z^2/yz}$ | 0.00 | 1.088 | 0.00 | 0.00 | 0.00 | 2.751 | 0.00 | 0.00 | 0.00 | 0.0 | 0.00 |
| $P_{z^2/x^2-y^2}$ | 0.00 | 0.00 | −2.177 | 0.00 | 0.00 | 0.00 | 1.919 | 0.00 | 0.00 | 0.0 | 0.00 |
| $P_{z^2/xy}$ | 0.00 | 0.00 | 0.00 | −2.177 | 0.00 | 0.00 | 0.00 | 1.919 | 0.00 | 0.0 | 0.00 |
| $P_{xz/yz}$ | 0.00 | 0.00 | 0.00 | 1.885 | 0.00 | 0.00 | 0.00 | 2.216 | 0.00 | 0.0 | 0.00 |
| $P_{xz/x^2-y^2}$ | 1.885 | 0.00 | 0.00 | 0.00 | −0.794 | 0.00 | 0.00 | 0.00 | 2.094 | 0.0 | 0.00 |
| $P_{xz/xy}$ | 0.00 | 1.885 | 0.00 | 0.00 | 0.00 | −0.794 | 0.00 | 0.00 | 0.00 | 2.094 | 0.00 |
| $P_{yz/x^2-y^2}$ | 0.00 | −1.885 | 0.00 | 0.00 | 0.00 | 0.794 | 0.00 | 0.00 | 0.00 | 2.094 | 0.00 |
| $P_{yz/xy}$ | 1.885 | 0.00 | 0.00 | 0.00 | −0.794 | 0.00 | 0.00 | 0.00 | −2.094 | 0.00 | 0.00 |
| $P_{x^2-y^2/xy}$ | 0.00 | 0.00 | 0.00 | 0.00 | 0.00 | 0.00 | 0.00 | 0.00 | 0.00 | 0.00 | 3.142 |

$$\begin{array}{ccccccc} \text{electrostatic properties} & & & & & & \\ \uparrow & & & & & & \\ \rho(\mathbf{r}) & \leftarrow & \langle\rho(\mathbf{r})\rangle & \leftarrow & F(\mathbf{h}) & \leftarrow & I(\mathbf{h}) \\ \downarrow & & \downarrow & & & & \\ \Delta\rho(\mathbf{r}) & \leftarrow & \langle\Delta\rho(\mathbf{r})\rangle. & & & & \end{array} \tag{8.7.3.75}$$

The crucial step in each sequence is the thermal averaging (top sequence) or the deconvolution of thermal motion (bottom sequence), which in principle requires detailed knowledge of both the internal (molecular) and the external (lattice) modes of the crystal. Even within the generally accepted Born–Oppenheimer approximation, this is a formidable task, which can be simplified for molecular crystals by the assumption that the thermal smearing is dominated by the larger-amplitude external modes. The procedure (8.7.3.65) requires an adequate thermal-motion model in the structure-factor formalism applied to the experimental structure amplitudes. The commonly used models may include anharmonicity, as described in Volume B, Chapter 1.2 (*IT*B, 1992), but assume that a density function centred on an atom can be assigned the thermal motion of that atom, which may be a poor approximation for the more diffuse functions.

The missing link in scheme (8.7.3.75) is the sequence $\psi \leftarrow \Gamma^1(1,1) \leftarrow \rho(\mathbf{r})$. In order to describe the wavefunction analytically, a basis set is required. The number of coefficients in the wavefunction is minimized by the use of a minimal basis for the molecular orbitals, but calculations in general lead to poor-quality electron densities.

If the additional approximation is made that the wavefunction is a single Slater determinant, the idempotency condition can be used in the derivation of the wavefunction from the electron density. A simplified two-valence-electron two-orbital system has been treated in this manner (Massa, Goldberg, Frishberg, Boehme & La Placa, 1985), and further developments may be expected.

A special case occurs if the overlap between the orbitals on an atom and its neighbours is very small. In this case, a direct relation can be derived between the populations of a minimal basis set of valence orbitals and the multipole coefficients, as described in the following sections.

### 8.7.3.6. *Occupancies of transition-metal valence orbitals from multipole coefficients*

In general, the atom-centred density model functions describe both the valence and the two-centre overlap density. In the case of transition metals, the latter is often small, so that to a good approximation the atomic density can be expressed in terms of an atomic orbital basis set $d_i$, as well as in terms of the multipolar expansion. Thus,

$$\begin{aligned} \rho_d &= \sum_{i=1}^{5}\sum_{j\geq i}^{5} P_{ij} d_i d_j, \\ &= \sum_{l=0}^{4} \kappa'^3 \left\{ R_l(\kappa' r) \sum_{m=0}^{l}\sum_{p} P_{lmp} d_{lmp} \right\}, \end{aligned} \tag{8.7.3.76}$$

in which $d_{lmp}$ are the density functions.

The orbital products $d_i d_j$ can be expressed as linear combinations of spherical harmonic functions, with coefficients listed in Volume B, Chapter 1.2 (*IT*B, 1992), which leads to relations between the $P_{ij}$ and $P_{lmp}$. In matrix notation,

$$\mathbf{P}_{lmp} = \boldsymbol{M}\mathbf{P}_{ij}, \tag{8.7.3.77}$$

where $\mathbf{P}_{lmp}$ is a vector containing the coefficients of the 15 spherical harmonic functions with $l = 0$, 2, or 4 that are generated by the products of $d$ orbitals. The matrix $\boldsymbol{M}$ is also a function of the ratio of orbital and density-function normalization coefficients, given in Volume B, Chapter 1.2 (*IT*B, 1992).

Table 8.7.3.4. *Orbital–multipole relations for square-planar complexes (point group $D_{4h}$)*

| | | $P_{00}$ | $P_{20}$ | $P_{40}$ | $P_{44+}$ |
|---|---|---|---|---|---|
| $P_{20}$ | $a_{1g}$ | 0.200 | 1.039 | 1.396 | 0.00 |
| $P_{21+}$ | $e_g$ | 0.200 | 0.520 | −0.931 | 0.00 |
| $P_{21-}$ | | 0.200 | 0.520 | −0.931 | 0.00 |
| $P_{22+}$ | $b_{1g}$ | 0.200 | −1.039 | 0.233 | 1.570 |
| $P_{22}$ | $b_{2g}$ | 0.200 | −1.039 | 0.233 | −1.570 |

The $d$-orbital occupancies can be derived from the experimental multipole populations by the inverse expression,

$$\mathbf{P}_{ij} = \boldsymbol{M}^{-1}\mathbf{P}_{lmp} \tag{8.7.3.78}$$

(Holladay, Leung & Coppens, 1983).

The matrix $\boldsymbol{M}^{-1}$ is given in Table 8.7.3.3. Point-group-specific expressions can be derived by omission of symmetry-forbidden terms. Matrices for point group $4/mmm$ (square planar) and for trigonal point groups ($\bar{3}$, $\bar{3}$, 32, $3m$, $\bar{3}m$) are listed in Tables 8.7.3.4 and 8.7.3.5, respectively. Point groups with and without vertical mirror planes are distinguished by the occurrence of both $d_{lm+}$ and $d_{lm-}$ functions in the latter case, and only $d_{lm+}$ in the former, with $m$ being restricted to $n$, the order of the rotation axis. The $d_{ln-}$ functions can be eliminated by rotation of the coordinate system around a vertical axis through an angle $\psi_0$ given by $\psi_0 = (1/n)\arctan(P_{ln-}/P_{ln+})$.

### 8.7.3.7. *Thermal smearing of theoretical densities*

#### 8.7.3.7.1. *General considerations*

In the Born–Oppenheimer approximation, the electrons rearrange instantaneously to the minimum-energy state for each nuclear configuration. This approximation is generally valid, except when very low lying excited electronic states exist. The thermally smeared electron density is then given by

$$\langle\rho(\mathbf{r})\rangle = \int \rho(\mathbf{r}, \mathbf{R})P(\mathbf{R})\,\mathrm{d}(\mathbf{R}), \tag{8.7.3.79}$$

where $\mathbf{R}$ represents the $3N$ nuclear space coordinates and $P(\mathbf{R})$ is the probability of the configuration $\mathbf{R}$. Evaluation of (8.7.3.79) is possible if the vibrational spectrum is known, but requires a large number of quantum-mechanical calculations at points along the vibrational path. A further approximation is the convolution approximation, which assumes that the charge density near each nucleus can be convoluted with the vibrational motion of that nucleus,

$$\langle\rho(\mathbf{r})\rangle = \sum_n \int \rho_n(\mathbf{r} - \mathbf{u} - \mathbf{R}_n)P_n(\mathbf{u})\,\mathrm{d}\mathbf{u}, \tag{8.7.3.80}$$

where $\rho_n$ stands for the density of the $n$th pseudo-atom. The convolution approximation thus requires decomposition of the density into atomic fragments. It is related to the thermal-motion formalisms commonly used, and requires that two-centre terms in the theoretical electron density be either projected into the atom-centred density functions, or assigned the thermal motion of a point between the two centres. In the LCAO approximation (8.7.3.9), the two-centre terms are represented by

$$\rho_{\mu\nu}(\mathbf{r}) = P_{\mu\nu}\chi_\mu(\mathbf{r} - \mathbf{R}_\mu)\chi_\nu(\mathbf{r} - \mathbf{R}_\nu), \tag{8.7.3.81}$$

where $\chi_\mu$ and $\chi_\nu$ are basis functions centred at $\mathbf{R}_\mu$ and $\mathbf{R}_\nu$, respectively. As the motion of a point between the two vibrating atoms depends on their relative phase, further assumptions must be made. The simplest is to assume a gradual variation of the thermal motion along the bond, which gives at a point $\mathbf{r}_i$ on the internuclear vector of length $R_{\mu\nu}$

$$U_{ij}(\mathbf{r}_i) = \left[U_{ij}(\mathbf{R}_\mu)\left|\mathbf{R}_\mu - \mathbf{r}_i\right| + U_{ij}(\mathbf{R}_\nu)\left|\mathbf{R}_\nu - \mathbf{r}_i\right|\right]/R_{\mu\nu}. \tag{8.7.3.82}$$

This expression may be used to assign thermal parameters to a bond-centred function.

Table 8.7.3.5. *Orbital–multipole relations for trigonal complexes*

| | $P_{00}$ | $P_{2-}$ | $P_{40}$ | $P_{43+}$ | $P_{43-}$ |
|---|---|---|---|---|---|
| (*a*) In terms of $d$ orbitals | | | | | |
| $P_{20}$ | 0.200 | 1.039 | 1.396 | 0.00 | 0.00 |
| $P_{21+}$ | 0.200 | 0.520 | −0.931 | 0.00 | 0.00 |
| $P_{21-}$ | 0.200 | 0.520 | −0.931 | 0.00 | 0.00 |
| $P_{22+}$ | 0.200 | −1.039 | 0.233 | 0.00 | 0.00 |
| $P_{22-}$ | 0.200 | −1.039 | 0.233 | 0.00 | 0.00 |
| $P_{21+/22+}$ | 0.00 | 0.00 | 0.00 | 2.094 | 0.00 |
| $P_{21+/22-}$ | 0.00 | 0.00 | 0.00 | 0.00 | 2.094 |
| $P_{21-/22+}$ | 0.00 | 0.00 | 0.00 | 0.00 | 2.094 |
| $P_{21-/22-}$ | 0.00 | 0.00 | 0.00 | −2.094 | 0.00 |
| (*b*) In terms of symmetry-adapted orbitals*† | | | | | |
| $P_1(a_{1g})$ | 0.200 | 1.039 | 1.396 | 0.00 | |
| $P_2(e_g)$ | 0.400 | −1.039 | −0.310 | −1.975 | |
| $P_3(e'_g)$ | 0.400 | 0.00 | −1.087 | 1.975 | |
| $P_4(e_{g^+}e'_g + e_{g^-}e'_{g^-})$ | 0.00 | −2.942 | 2.193 | 1.397 | |

* The electron density in terms of the symmetry-adapted orbitals is given by:

$$\rho_{3d} = P_1a_{1g}^2 + \tfrac{1}{2}P_2(e_{g^+}^2 - e_{g^-}^2) + \tfrac{1}{2}P_4(e_{g^+}e'_g + e_{g^-}e'_{g^-}),$$

with: $a_{1g} = d_{z^2}$; $e_{g^+} = \sqrt{(2/3)}d_{x^2-y^2} - \sqrt{(1/3)}d_{xz}$; $e_{g^-} = \sqrt{(2/3)}d_{xy} + \sqrt{(1/3)}d_{yz}$; $e'_{g^+} = \sqrt{(1/3)}d_{x^2-y^2} + \sqrt{(2/3)}d_{xz}$; and $e'_{g^-} = \sqrt{(1/3)}d_{xy} - \sqrt{(2/3)}d_{yz}$. † The signs given here imply a positive $e'_g$ lobe in the positive $xz$ quadrant. Care should be exercised in defining the coordinate system if this lobe is to point towards a ligand atom.

#### 8.7.3.7.2. *Reciprocal-space averaging over external vibrations*

Thermal averaging of the electron density is considerably simplified for modes in which adjacent atoms move in phase. In molecular crystals, such modes correspond to rigid-body vibrations and librations of the molecule as a whole. Their frequencies are low because of the weakness of intermolecular interactions. Rigid-body motions therefore tend to dominate thermal motion, in particular at temperatures for which $kT$ ($k = 0.7\ \mathrm{cm}^{-1}$) is large compared with the spacing of the vibrational energy levels of the external modes (internal modes are typically not excited to any extent at or below room temperature).

For a translational displacement ($\mathbf{u}$), the dynamic density is given by

$$\rho_{\mathrm{dyn}}(\mathbf{r}) = \int \rho(\mathbf{r} - \mathbf{u})P(\mathbf{u})\,\mathrm{d}\mathbf{u}, \tag{8.7.3.83}$$

with $\rho(\mathbf{r})$ defined by (8.7.3.81) (Stevens, Rees & Coppens, 1977). In the harmonic approximation, $P(\mathbf{u})$ is a normalized three-dimensional Gaussian probability function, the exponents

of which may be obtained by rigid-body analysis of the experimental data. In general, for a translational displacement (**u**) and a librational oscillation ($\omega$),

$$\rho_{\rm dyn}(\mathbf{r}) = \left(\sum P_{\mu\nu}\chi_\mu\chi_\nu\right) * P(\mathbf{u},\omega). \tag{8.7.3.84}$$

If correlation between **u** and $\omega$ can be ignored (neglect of the screw tensor **S**), $P(\mathbf{u},\omega) = P(\mathbf{u})P(\omega)$, and both types of modes can be treated independently. For the translations

$$\begin{aligned}\langle\rho\rangle_{\rm trans} &= \sum P_{\mu\nu}\left\{\chi_\mu(\mathbf{r})\chi_\nu(\mathbf{r}) * P(\mathbf{u})\right\}\\ &= \sum P_{\mu\nu}F^{-1}\left\{f_{\mu\nu}(\mathbf{h})\cdot T_{\rm tr}(\mathbf{h})\right\},\end{aligned} \tag{8.7.3.85}$$

where $F^{-1}$ is the inverse Fourier transform operator, and $T_{\rm tr}(\mathbf{h})$ is the translational temperature factor.

If $\boldsymbol{R}$ is an orthogonal rotation matrix corresponding to a rotation $\omega$, we obtain for the librations

$$\begin{aligned}\langle\rho\rangle_{\rm libr} &= \sum P_{\mu\nu}\left\{\chi_\mu(\boldsymbol{R}\mathbf{r})\chi_\nu(\boldsymbol{R}\mathbf{r}) * P(\omega)\right\}\\ &= \sum P_{\mu\nu}F^{-1}\left\{\left\langle f_{\mu\nu}(\boldsymbol{R}\mathbf{h})\right\rangle\right\},\end{aligned} \tag{8.7.3.86}$$

in which $f(\mathbf{h})$ has been averaged over the distribution of orientations of **h** with respect to the molecule;

$$\left\langle f_{\mu\nu}(\mathbf{h})\right\rangle = \int f_{\mu\nu}(\boldsymbol{R}\mathbf{h})P(\omega)\,{\rm d}\omega. \tag{8.7.3.87}$$

Evaluation of (8.7.3.85) and (8.7.3.86) is most readily performed if the basis functions $\psi$ have a Gaussian-type radial dependence, or are expressed as a linear combination of Gaussian radial functions.

For Gaussian products of *s* orbitals, the molecular scattering factor of the product $\psi_\mu\psi_\nu = N_\mu\exp[-\alpha_\mu(\mathbf{r}-\mathbf{r}_A)^2]\times N_\nu\exp[-\alpha_\nu(\mathbf{r}-\mathbf{r}_B)^2]$, where $N_\mu$ and $N_\nu$ are the normalization factors of the orbitals $\mu$ and $\nu$ centred on atoms *A* and *B*, is given by

$$\begin{aligned}f^{s,s}_{\rm stat}(\mathbf{h}) = N_\mu N_\nu &\exp\left(-\frac{\alpha_\mu\alpha_\nu}{\alpha_\mu+\alpha_\nu}\left|\mathbf{r}_A-\mathbf{r}_B\right|^2\right)\left(\frac{\pi}{\alpha_\mu+\alpha_\nu}\right)^{3/2}\\ &\times\exp\left(\frac{-\pi^2|h|^2}{\alpha_\mu+\alpha_\nu}\right)\exp(2\pi i\mathbf{h}\cdot\mathbf{r}_c),\end{aligned} \tag{8.7.3.88}$$

where the centre of density $\mathbf{r}_c$ is defined by $\mathbf{r}_c = (\alpha_\mu\mathbf{r}_A+\alpha_\nu\mathbf{r}_B)/(\alpha_\mu+\alpha_\nu)$.

For the translational modes, the temperature-factor exponent $-2\pi^2\sum_i\sum_j U_{ij}h_ih_j$ is simply added to the Gaussian exponent in (8.7.3.88) to give

$$\exp\left(-\frac{\pi^2|h|^2}{\alpha_\mu+\alpha_\nu}\right) - 2\pi^2\sum_i\sum_j U_{ij}h_ih_j.$$

For librations, we may write

$$\boldsymbol{R}\mathbf{r} = \mathbf{r} + \mathbf{u}_{\rm lib}$$

As $(\boldsymbol{R}\mathbf{h})\cdot\mathbf{r} = \mathbf{h}\cdot\boldsymbol{R}^T\mathbf{r} = \mathbf{h}\cdot\mathbf{r} - (\boldsymbol{R}\mathbf{h})\cdot\mathbf{u}_{\rm lib}$, for a function centred at **r**,

$$\begin{aligned}\left\langle\exp(2\pi\mathbf{h}\cdot\mathbf{r}_c)\right\rangle &= \sum\exp\left[2\pi i(\boldsymbol{R}\mathbf{h})\cdot\mathbf{r}_c\right]P(\delta)\,{\rm d}\omega\\ &= \exp(2\pi\mathbf{h}\cdot\mathbf{r}_c)\int\exp\left[-2\pi i(\boldsymbol{R}\mathbf{h})\cdot\mathbf{u}^c_{\rm lib}\right]P(\omega)\,{\rm d}\omega,\end{aligned} \tag{8.7.3.89}$$

which shows that for *ss* orbital products the librational temperature factor can be factored out, or

$$f^{s,s}_{\rm dyn} = f^{s,s}_{\rm stat}\int\exp\left[-2\pi i(\boldsymbol{R}\mathbf{h})\cdot\mathbf{u}^c_{\rm lib}\right]P(\omega)\,{\rm d}\omega. \tag{8.7.3.90}$$

Expressions for $P(\omega)$ are described elsewhere (Pawley & Willis, 1970).

For general Cartesian Gaussian basis functions of the type

$$\psi(\mathbf{r}) = (x-x_A)^m(y-y_A)^n(z-z_A)^p\exp(-\alpha|\mathbf{r}-\mathbf{r}_A|^2), \tag{8.7.3.91}$$

the scattering factors are more complicated (Miller & Krauss, 1967; Stevens, Rees & Coppens, 1977), and the librational temperature factor can no longer be factored out. However, it may be shown that, to a first approximation, (8.7.3.90) can again be used. This 'pseudotranslation' approximation corresponds to a neglect of the change in orientation (but not of position) of the two-centre density function and is adequate for moderate vibrational amplitudes.

Thermally smeared density functions are obtained from the averaged reciprocal-space function by performing the inverse Fourier transform with phase factors depending on the position coordinates of each orbital product

$$\langle\rho\rangle = \frac{1}{V}\sum P_{\mu\nu}\sum_{\mathbf{h}} f_{\mu\nu}(\mathbf{h})\exp\left[-2\pi i\mathbf{h}\cdot(\mathbf{r}-\mathbf{r}_c)\right], \tag{8.7.3.92}$$

where the orbital product $\chi_\mu\chi_\nu$ is centred at $\mathbf{r}_c$. If the summation is truncated at the experimental limit of $(\sin\theta)/\lambda$, both thermal vibrations and truncation effects are properly introduced in the theoretical densities.

### 8.7.3.8. *Uncertainties in experimental electron densities*

It is often important to obtain an estimate of the uncertainty in the deformation densities in Table 8.7.3.1. If it is assumed that the density of the static atoms or fragments that are subtracted out are precisely known, three sources of uncertainty affect the deformation densities: (1) the uncertainties in the experimental structure factors; (2) the uncertainties in the positional and thermal parameters of the density functions that influence $\rho_{\rm calc}$; and (3) the uncertainty in the scale factor *k*.

If we assume that the uncertainties in the observed structure factors are not correlated with the uncertainties in the refined parameters, the variance of the electron density is given by

$$\begin{aligned}\sigma^2(\Delta\rho) = \sigma^2\left(\rho'_{\rm obs}\right) + \sigma^2\left(\rho_{\rm calc}\right) + \left(\rho'_{\rm obs}\right)^2\frac{\sigma^2(k)}{k^2}\\ + \sum_p\frac{\delta\rho_{\rm calc}}{\delta u_p}\sigma\left(u_p\right)\rho'_{\rm obs}\frac{\sigma(k)}{k}\gamma\left(u_p,k\right),\end{aligned} \tag{8.7.3.93}$$

where $\rho'_{\rm obs} = \rho_{\rm obs}/k$, $u_p$ is a positional or thermal parameter, and the $\gamma(u_p,k)$ are correlation coefficients between the scale factor and the other parameters (Rees, 1976, 1978; Stevens & Coppens, 1976).

Similarly, for the covariance between the deformation densities at points *A* and *B*,

$$\begin{aligned}{\rm cov}(\Delta\rho_A,\Delta\rho_B) = {\rm cov}\left(\rho_{{\rm obs},A},\rho_{{\rm obs},B}\right)/k^2\\ + {\rm cov}\left(\rho_{{\rm calc},A},\rho_{{\rm calc},B}\right)\\ + \rho_{{\rm obs},A}\rho_{{\rm obs},B}[\sigma(k)/k]^2,\end{aligned} \tag{8.7.3.94}$$

where it is implied that the second term includes the effect of the scale factor/parameter correlation.

Following Rees (1976), we may derive a simplified expression for the covariance valid for the space group $P\bar{1}$. Since the structure factors are not correlated with each other,

$$\operatorname{cov}\left(\rho_{\mathrm{obs},A}, \rho_{\mathrm{obs},B}\right) \simeq \sum \frac{\partial \rho_{\mathrm{obs},A}}{\partial F_{\mathrm{obs}}(\mathbf{h})} \frac{\partial \rho_{\mathrm{obs},B}}{\partial F_{\mathrm{obs}}(\mathbf{h})} \sigma^2\left[F_{\mathrm{obs}}(\mathbf{h})\right]$$
$$\simeq \frac{2}{V^2} \sum_{1/2} \sigma^2(F_{\mathrm{obs}}) \left[\cos 2\pi(\mathbf{r}_A + \mathbf{r}_B)\cdot\mathbf{h} + \cos 2\pi(\mathbf{r}_A - \mathbf{r}_B)\cdot\mathbf{h}\right], \quad (8.7.3.95)$$

where the latter equality is specific for $P\bar{1}$, and $\sum_{1/2}$ indicates summation over a hemisphere in reciprocal space. In general, the second term rapidly averages to zero as $h_{\max}$ increases, while the first term may be replaced by its average

$$\left\langle \cos 2\pi(\mathbf{r}_A - \mathbf{r}_B)\cdot\mathbf{h} \right\rangle = 3(\sin u - u\cos u)/u^3 \equiv \mathrm{C}(u), \quad (8.7.3.96)$$

with $u = 2\pi|\mathbf{r}_A - \mathbf{r}_B|h_{\max}$, or $\operatorname{cov}(\rho_{\mathrm{obs},A}\rho_{\mathrm{obs},B}) \simeq (2/V^2)C(u) \times \sum_{1/2}\sigma^2(F_0)$ and $\sigma^2(\rho_{\mathrm{obs}}) \simeq (2/V^2)\sum_{1/2}\sigma^2(F_0)$, a relation derived earlier by Cruickshank (1949). A discussion of the applicability of this expression in other centrosymmetric space groups is given by Rees (1976).

#### 8.7.3.9. *Uncertainties in derived functions*

The electrostatic moments are functions of the scale factor, the positional parameters $x$, $y$ and $z$ of the atoms, and their charge-density parameters $\kappa$ and $P_{lmp}$. The standard uncertainties in the derived moments are therefore dependent on the variances and covariances of these parameters.

If $\boldsymbol{M}_p$ represents the $m \times m$ variance–covariance matrix of the parameters $p_j$, and $\boldsymbol{T}$ is an $n \times m$ matrix defined by $\partial\mu^l/\partial p_j$ for the $l$th moment with $n$ independent elements, the variances and covariances of the elements of $m^l$ are obtained from

$$\boldsymbol{M}_\mu = \boldsymbol{T}\boldsymbol{M}_p\boldsymbol{T}^T. \quad (8.7.3.96a)$$

If a moment of an assembly of pseudo-atoms is evaluated, the elements of $\boldsymbol{T}$ include the effects of coordinate rotations required to transfer atomic moments into a common coordinate system.

A frequently occurring case of interest is the evaluation of the magnitude of a molecular dipole moment and its standard deviation. Defining

$$y = \mu^2 = \boldsymbol{\mu}\boldsymbol{G}\boldsymbol{\mu}^T, \quad (8.7.3.96b)$$

where $\boldsymbol{\mu}$ is the dipole-moment vector and $\boldsymbol{G}$ is the direct-space metric tensor of the appropriate coordinate system. If $\boldsymbol{Y}$ is the $1 \times 3$ matrix of the derivatives $\partial y/\partial\mu_i$,

$$\sigma^2(y) = \boldsymbol{Y}\boldsymbol{M}_\mu\boldsymbol{Y}^T, \quad (8.7.3.96c)$$

where $\boldsymbol{M}_\mu$ is defined by (8.7.3.96*a*). The standard uncertainty in $\mu$ may be obtained from $\sigma(\mu) = \sigma(y)/2\mu$. Significant contributions often result from uncertainties in the positional and charge-density parameters of the H atoms.

### 8.7.4. Spin densities

#### 8.7.4.1. *Introduction*

Magnetism and magnetic ordering are among the central problems in condensed-matter research. One of the main issues in macroscopic studies of magnetism is a description of the magnetization density $\boldsymbol{\mu}$ as a function of temperature and applied field: phase diagrams can be explained from such studies.

Diffraction techniques allow determination of the same information, but at a microscopic level. Let $\mathbf{m}(\mathbf{r})$ be the microscopic magnetization density, a function of the position $\mathbf{r}$ in the unit cell (for crystalline materials). Macroscopic and microscopic magnetization densities are related by the simple expression

$$\boldsymbol{\mu} = \frac{1}{V}\int_{\mathrm{cell}} \mathbf{m}(\mathbf{r})\,\mathrm{d}\mathbf{r}, \quad (8.7.4.1)$$

where $V$ is the volume of the unit cell, $\mathbf{m}(\mathbf{r})$ is the sum of two contributions: $\mathbf{m}_s(\mathbf{r})$ originating from the spins of the electrons, and $\mathbf{m}_L(\mathbf{r})$ originating from their orbital motion.

$$\mathbf{m}(\mathbf{r}) = \mathbf{m}_s(\mathbf{r}) + \mathbf{m}_L(\mathbf{r}). \quad (8.7.4.2)$$

#### 8.7.4.2. *Magnetization densities from neutron magnetic elastic scattering*

The scattering process is discussed in Section 6.1.3 and only the features that are essential to the present chapter will be summarized here.

For neutrons, the nuclear structure factor $F_N(\mathbf{h})$ is given by

$$F_N(\mathbf{h}) = \sum_j b_j T_j \exp(2\pi i\mathbf{h}\cdot\mathbf{R}_j). \quad (8.7.4.3)$$

$b_j$, $T_j$, $\mathbf{R}_j$ are the coherent scattering length, the temperature factor, and the equilibrium position of the $j$th atom in the unit cell.

Let $\boldsymbol{\sigma}$ be the spin of the neutron (in units of $\hbar/2$). There is a dipolar interaction of the neutron spin with the electron spins and the currents associated with their motion. The magnetic structure factor can be written as the scalar product of the neutron spin and an 'interaction vector' $\mathbf{Q}(\mathbf{h})$:

$$F_M(\mathbf{h}) = \boldsymbol{\sigma}\cdot\mathbf{Q}(\mathbf{h}). \quad (8.7.4.4)$$

$\mathbf{Q}(\mathbf{h})$ is the sum of a spin and an orbital term: $\mathbf{Q}_s$ and $\mathbf{Q}_L$, respectively. If $r_0 = \gamma r_e \sim 0.54 \times 10^{-12}$ cm, where $\gamma$ is the gyromagnetic factor ($=1.913$) of the neutron and $r_e$ the classical Thomson radius of the electron, the spin term is given by

$$\mathbf{Q}_s(\mathbf{h}) = r_0\hat{\mathbf{h}} \times \mathbf{M}_s(\mathbf{h}) \times \hat{\mathbf{h}}, \quad (8.7.4.5)$$

$\hat{\mathbf{h}}$ being the unit vector along $\mathbf{h}$, while $\mathbf{M}_s(\mathbf{h})$ is defined as

$$\mathbf{M}_s(\mathbf{h}) = \left\langle \sum_j \boldsymbol{\sigma}_j \exp(2\pi i\mathbf{h}\cdot\mathbf{r}_j) \right\rangle, \quad (8.7.4.6)$$

where $\boldsymbol{\sigma}_j$ is the spin of the electron at position $\mathbf{r}_j$, and angle brackets denote the ensemble average over the scattering sample. $\mathbf{M}_s(\mathbf{h})$ is the Fourier transform of the spin-magnetization density $\mathbf{m}_s(\mathbf{r})$, given by

$$\mathbf{m}_s(\mathbf{r}) = \left\langle \sum_j \boldsymbol{\sigma}_j \delta(\mathbf{r} - \mathbf{r}_j) \right\rangle. \quad (8.7.4.7)$$

This is the spin-density vector field in units of $2\mu_B$.

The orbital part of $\mathbf{Q}(\mathbf{h})$ is given by

$$\mathbf{Q}_L(\mathbf{h}) = -\frac{ir_0}{2\pi h}\hat{\mathbf{h}} \times \left\langle \sum_j \mathbf{p}_j \exp(2\pi i\mathbf{h}\cdot\mathbf{r}_j) \right\rangle, \quad (8.7.4.8)$$

where $\mathbf{p}_j$ is the momentum of the electrons. If the current density vector field is defined by

$$\mathbf{j}(\mathbf{r}) = -\frac{e}{2m}\left\langle \sum_j \left\{\mathbf{p}_j\delta(\mathbf{r} - \mathbf{r}_j) + \delta(\mathbf{r} - \mathbf{r}_j)\mathbf{p}_j\right\} \right\rangle, \quad (8.7.4.9)$$

$\mathbf{Q}_L(\mathbf{h})$ can be expressed as

$$\mathbf{Q}_L(\mathbf{h}) = -\frac{ir_0}{2\pi h}\hat{\mathbf{h}} \times \mathbf{J}(\mathbf{h}), \quad (8.7.4.10)$$

where $\mathbf{J}(\mathbf{h})$ is the Fourier transform of the current density $\mathbf{j}(\mathbf{r})$.

The electrodynamic properties of $\mathbf{j}(\mathbf{r})$ allow it to be written as the sum of a rotational and a nonrotational part:

$$\mathbf{j}(\mathbf{r}) = \nabla\psi + \nabla \times [\mathbf{m}_L(\mathbf{r})], \tag{8.7.4.11}$$

where $\nabla\psi$ is a 'conduction' component and $\mathbf{m}_L(\mathbf{r})$ is an 'orbital-magnetization' density vector field.

Substitution of the Fourier transform of (8.7.4.11) into (8.7.4.10) leads in analogy to (8.7.4.5) to

$$\mathbf{Q}_L(\mathbf{h}) = r_0 \hat{\mathbf{h}} \times \mathbf{M}_L(\mathbf{h}) \times \hat{\mathbf{h}}, \tag{8.7.4.12}$$

where $\mathbf{M}_L(\mathbf{h})$ is the Fourier transform of $\mathbf{m}_L(\mathbf{r})$. The rotational component $\nabla\psi$ of $\mathbf{j}(\mathbf{r})$ does not contribute to the neutron scattering process. It is therefore possible to write $\mathbf{Q}(\mathbf{h})$ as

$$\mathbf{Q}(\mathbf{h}) = r_0 \hat{\mathbf{h}} \times \mathbf{M}(\mathbf{h}) \times \hat{\mathbf{h}}, \tag{8.7.4.13}$$

with

$$\mathbf{M}(\mathbf{h}) = \mathbf{M}_s(\mathbf{h}) + \mathbf{M}_L(\mathbf{h}) \tag{8.7.4.14}$$

being the Fourier transform of the 'total' magnetization density vector field, and

$$\mathbf{m}(\mathbf{r}) = \mathbf{m}_s(\mathbf{r}) + \mathbf{m}_L(\mathbf{r}). \tag{8.7.4.15}$$

As $\mathbf{Q}(\mathbf{h})$ is the projection of $\mathbf{M}(\mathbf{h})$ onto the plane perpendicular to $\mathbf{h}$, there is no magnetic scattering when $\mathbf{M}$ is parallel to $\mathbf{h}$. It is clear from (8.7.4.13) that $\mathbf{M}(\mathbf{h})$ can be defined to any vector field $\mathbf{V}(\mathbf{h})$ parallel to $\mathbf{h}$, *i.e.* such that $\mathbf{h} \times \mathbf{V}(\mathbf{h}) = 0$.

This means that in real space $\mathbf{m}(\mathbf{r})$ is defined to any vector field $\mathbf{v}(\mathbf{r})$ such that $\nabla \times \mathbf{v}(\mathbf{r}) = 0$. Therefore, $\mathbf{m}(\mathbf{r})$ is defined to an arbitrary gradient.

As a result, magnetic neutron scattering cannot lead to a uniquely defined orbital magnetization density. However, the definition (8.7.4.7) for the spin component is unambiguous.

However, the integrated magnetic moment $\boldsymbol{\mu}$ is determined unambiguously and must thus be identical to the magnetic moment defined from the principles of quantum mechanics, as discussed in §8.7.4.5.1.3.

Before discussing the analysis of magnetic neutron scattering in terms of spin-density distributions, it is necessary to give a brief description of the quantum-mechanical aspects of magnetization densities.

### 8.7.4.3. *Magnetization densities and spin densities*

#### 8.7.4.3.1. *Spin-only density at zero temperature*

Let us consider first an isolated open-shell system, whose orbital momentum is quenched: it is a spin-only magnetism case. Let $\hat{\mathbf{m}}_s$ be the spin-magnetization-density operator (in units of $2\mu_B$):

$$\hat{\mathbf{m}}_s = \sum_j \hat{\boldsymbol{\sigma}}_j \, \delta(\mathbf{r} - \mathbf{r}_j). \tag{8.7.4.16}$$

$\mathbf{r}_j$ and $\hat{\boldsymbol{\sigma}}_j$ are, respectively, the position and the spin operator (in $\hbar$ units) of the $j$th electron. This definition is consistent with (8.7.4.7).

The system is assumed to be at zero temperature, under an applied field, the quantization axis being $Oz$. The ground state is an eigenstate of $\hat{\mathbf{S}}^2$ and $\hat{S}_z$, where $\hat{\mathbf{S}}$ is the total spin:

$$\hat{\mathbf{S}} = \sum_j \hat{\boldsymbol{\sigma}}_j. \tag{8.7.4.17}$$

Let $S$ and $M_s$ be the eigenvalues of $\hat{\mathbf{S}}^2$ and $\hat{S}_z$. ($M_s$ will in general be fixed by Hund's rule: $M_S = S$.)

$$2M_S = [n_\uparrow - n_\downarrow], \tag{8.7.4.18}$$

where $n_\uparrow$ and $n_\downarrow$ are the numbers of electrons with ($\uparrow$: $+\frac{1}{2}$) and ($\downarrow$: $-\frac{1}{2}$) spin, respectively.

The spin-magnetization density is along $\mathbf{z}$, and is given by

$$m_{Sz}(\mathbf{r}) = \left\langle \psi_{SM_S} \left| \sum_j \hat{\boldsymbol{\sigma}}_{jz} \, \delta(\mathbf{r} - \mathbf{r}_j) \right| \psi_{SM_S} \right\rangle. \tag{8.7.4.19}$$

$m_{Sz}(\mathbf{r})$ is proportional to the normalized spin density that was defined for a pure state in (8.7.2.10).

$$m_{Sz}(\mathbf{r}) = M_S s(\mathbf{r}). \tag{8.7.4.20}$$

If $\rho_\uparrow(\mathbf{r})$ and $\rho_\downarrow(\mathbf{r})$ are the charge densities of electrons of a given spin, the normalized spin density is defined as

$$s(\mathbf{r}) = [\rho_\uparrow(\mathbf{r}) - \rho_\downarrow(\mathbf{r})] \frac{1}{[n_\uparrow - n_\downarrow]}, \tag{8.7.4.21}$$

compared with the total charge density $\rho(\mathbf{r})$ given by

$$\rho(\mathbf{r}) = \rho_\uparrow(\mathbf{r}) + \rho_\downarrow(\mathbf{r}). \tag{8.7.4.22}$$

A strong complementarity is thus expected from joint studies of $\rho(\mathbf{r})$ and $s(\mathbf{r})$.

In the particular case of an independent electron model,

$$\rho_\alpha(\mathbf{r}) = \sum_{i=1}^{N_\alpha} |\varphi_{i\alpha}(\mathbf{r})|^2 \quad (\alpha = \uparrow, \downarrow), \tag{8.7.4.23}$$

where $\varphi_{i\alpha}(\mathbf{r})$ is an occupied orbital for a given spin state of the electron.

If the ground state is described by a correlated electron model (mixture of different configurations), the one-particle reduced density matrix can still be analysed in terms of its eigenvectors $\psi_{i\alpha}$ and eigenvalues $n_{i\alpha}$ (natural spin orbitals and natural occupancies), as described by the expression

$$\rho_\alpha(\mathbf{r}) = \sum_{i=1}^{\infty} n_{i\alpha} |\psi_{i\alpha}(\mathbf{r})|^2, \tag{8.7.4.24}$$

where $\langle \psi_{i\alpha} | \psi_{j\beta} \rangle = \delta_{ij}\delta_{\alpha\beta}$, since the natural spin orbitals form an orthonormal set, and

$$n_{i\alpha} \leq 1 \quad \sum_{i=1}^{\infty} n_{i\alpha} = n_\alpha. \tag{8.7.4.25}$$

As the quantization axis is arbitrary, (8.7.4.20) can be generalized to

$$\mathbf{m}_s(\mathbf{r}) = \hat{\mathbf{S}} s(\mathbf{r}). \tag{8.7.4.26}$$

Equation (8.7.4.26) expresses the proportionality of the spin-magnetization density to the normalized spin density function.

#### 8.7.4.3.2. *Thermally averaged spin-only magnetization density*

The system is now assumed to be at a given temperature $T$. $S$ remains a good quantum number, but all ($SM_S$) states ($M_S = -S, \ldots, S$) are now populated according to Boltzmann statistics. We are interested in the thermal equilibrium spin-magnetization density:

$$\mathbf{m}_s(\mathbf{r}) = \sum_{M_S=-S}^{+S} p(M_S) \langle \psi_{SM_S} | \hat{\mathbf{m}}_s | \psi_{SM_S} \rangle, \tag{8.7.4.27}$$

where $p(M_S)$ is the population of the $M_S$ state. The operator $\hat{\mathbf{m}}_s$ fulfils the requirements to satisfy the Wigner–Eckart theorem (Condon & Shortley, 1935), which states that, within the $S$ manifold, all matrix elements of $\hat{\mathbf{m}}_s$ are proportional to $\hat{\mathbf{S}}$. The consequence of this remarkable property is that

$$\langle\psi_{SM_S}|\hat{\mathbf{m}}_s|\psi_{SM_S}\rangle = \langle\psi_{SM_S}|\hat{\mathbf{S}}|\psi_{SM_S}\rangle f_S(\mathbf{r}), \tag{8.7.4.28}$$

where $f_S(\mathbf{r})$ is a function that depends on $S$, but not on $M_S$. Comparison with (8.7.4.26) shows that $f_S(\mathbf{r})$ is the normalized spin-density function $s(\mathbf{r})$, which therefore is an invariant for the $S$ manifold [$s(\mathbf{r})$ is calculated as the normalized spin density for any $M_S$]. Expression (8.7.4.27) can thus be written as

$$\mathbf{m}_s(\mathbf{r}) = \langle\mathbf{S}\rangle s(\mathbf{r}), \tag{8.7.4.29}$$

where $\langle\mathbf{S}\rangle$ is the expected value for the total spin, at a given temperature and under a given external field. As $s(\mathbf{r})$ is normalized, the total moment of the system is

$$\boldsymbol{\mu}_S = \langle\mathbf{S}\rangle.$$

The behaviour of $\langle\mathbf{S}\rangle$ is governed by the usual laws of magnetism: it can be measured by macroscopic techniques. In paramagnetic species, it will vary as $T^{-1}$ to a first approximation; unless the system is studied at very low temperatures, the value of $\langle\mathbf{S}\rangle$ will be very small. The dependence of $\langle\mathbf{S}\rangle$ on temperature and orienting field is crucial.

Finally, (8.7.4.29) has to be averaged over vibrational modes. Except for the case where there is strong magneto-vibrational interaction, only $s(\mathbf{r})$ is affected by thermal atomic motion. This effect can be described in terms similar to those used for the charge density (Subsection 8.7.3.7).

The expression (8.7.4.29) is very important and shows that the microscopic spin-magnetization density carries two types of information: the nature of spin ordering in the system, described by $\langle\mathbf{S}\rangle$, and the delocalized nature of the electronic ground state, represented by $s(\mathbf{r})$.

#### 8.7.4.3.3. *Spin density for an assembly of localized systems*

A complex magnetic system can generally be described as an ensemble of well defined interacting open-shell subsystems (ions or radicals), where each subsystem has a spin $\hat{\mathbf{S}}_n$, and $S_n^2$ is assumed to be a good quantum number. The magnetic interaction occurs essentially through exchange mechanisms that can be described by the Heisenberg Hamiltonian:

$$\mathcal{H} = -\sum_{n<m} J_{nm}\,\hat{\mathbf{S}}_n \cdot \hat{\mathbf{S}}_m - \sum_n \mathbf{B}_0 \cdot \mathbf{S}_n, \tag{8.7.4.30}$$

where $J_{nm}$ is the exchange coupling between two subsystems, and $\mathbf{B}_0$ an applied external field (magneto-crystalline anisotropic effects may have to be added). Expression (8.7.4.30) is the basis for the understanding of magnetic ordering and phase diagrams. The interactions lead to a local field $\mathbf{B}_n$, which is the effective orienting field for the spin $\mathbf{S}_n$.

The expression for the spin-magnetization density is

$$\mathbf{m}_s(\mathbf{r}) = \sum_n \langle\mathbf{S}_n\rangle s_n(\mathbf{r}). \tag{8.7.4.31}$$

The relative arrangement of $\langle\mathbf{S}_n\rangle$ describes the magnetic structure; $s_n(\mathbf{r})$ is the normalized spin density of the $n$th subsystem.

In some metallic systems, at least part of the unpaired electron system cannot be described within a localized model: a band-structure description has to be used (Lovesey, 1984). This is the case for transition metals like Ni, where the spin-magnetization density is written as the sum of a localized part [described by (8.7.4.31)] and a delocalized part [described by (8.7.4.29)].

#### 8.7.4.3.4. *Orbital magnetization density*

We must now address the case where the orbital moment is not quenched. In that case, there is some spin-orbit coupling, and the description of the magnetization density becomes less straightforward.

The magnetic moment due to the angular momentum $\mathbf{l}_j$ of the electron is $\frac{1}{2}\mathbf{l}_j$ (in units of $2\mu_B$). As $\mathbf{l}_j$ does not commute with the position $\mathbf{r}_j$, orbital magnetization density is defined as

$$\mathbf{m}_L(\mathbf{r}) = \tfrac{1}{4}\left\langle \sum_j \{\mathbf{l}_j\,\delta(\mathbf{r}-\mathbf{r}_j) + \delta(\mathbf{r}-\mathbf{r}_j)\mathbf{l}_k\} \right\rangle. \tag{8.7.4.32}$$

If $\mathbf{L}$ is the total orbital moment,

$$\mathbf{L} = \sum_j \mathbf{l}_j. \tag{8.7.4.33}$$

Only open shells contribute to the orbital moment. But, in general, neither $\mathbf{L}^2$ nor $\mathbf{L}_z$ are constants of motion. There is, however, an important exception, when open-shell electrons can be described as localized around atomic centres. This is the case for most rare-earth compounds, for which the 4*f* electrons are too close to the nuclei to lead to a significant interatomic overlap. It can also be a first approximation for the *d* electrons in transition-metal ions. Spin-orbit coupling will be present, and thus only $\mathbf{L}^2$ will be a constant of motion. One may define the total angular momentum

$$\mathbf{J} = \mathbf{L} + \mathbf{S} \tag{8.7.4.34}$$

and $\{J^2, L^2, S^2, J_z\}$ become the four constants of motion.

Within the $J$ manifold of the ground state, $\mathbf{m}_s(\mathbf{r})$ and $\mathbf{m}_L(\mathbf{r})$ do not, in general, fulfil the conditions for the Wigner–Eckart theorem (Condon & Shortley, 1935), which leads to a very complex description of $\mathbf{m}(\mathbf{r})$ in practical cases.

However, the Wigner–Eckart theorem can be applied to the magnetic moments themselves, leading to

$$\mathbf{L} + 2\mathbf{S} = g\mathbf{J}, \tag{8.7.4.35}$$

with the Lande factor

$$g = 1 + \frac{J(J+1) - L(L+1) + S(S+1)}{2J(J+1)} \tag{8.7.4.36}$$

and, equivalently,

$$\begin{aligned} \mathbf{S} &= (g-1)\mathbf{J} \\ \mathbf{L} &= (2-g)\mathbf{J}. \end{aligned} \tag{8.7.4.37}$$

The influence of spin–orbit coupling on the scattering will be discussed in Subsection 8.7.4.5.

### 8.7.4.4. *Probing spin densities by neutron elastic scattering*

#### 8.7.4.4.1. *Introduction*

The magnetic structure factor $F_M(\mathbf{h})$ [equation (8.7.4.4)] depends on the spin state of the neutron. Let $\boldsymbol{\lambda}$ be the unit vector defining a quantization axis for the neutron, which can be either parallel ($\uparrow$) or antiparallel ($\downarrow$) to $\boldsymbol{\sigma}$. If $I_{\sigma\sigma'}$ stands for the cross section where the incident neutron has the polarization $\sigma$ and the scattered neutron the polarization $\sigma'$, one obtains the following basic expressions:

$$\begin{aligned} I_{\uparrow\uparrow} &= |F_n + \boldsymbol{\lambda}\cdot\mathbf{Q}|^2 \\ I_{\downarrow\downarrow} &= |F_n - \boldsymbol{\lambda}\cdot\mathbf{Q}|^2 \\ I_{\uparrow\downarrow} &= I_{\downarrow\uparrow} = |\boldsymbol{\lambda}\times\mathbf{Q}|^2. \end{aligned} \tag{8.7.4.38}$$

If no analysis of the spin state of the scattered beam is made, the two measurable cross sections are

$$I_\uparrow = I_{\uparrow\uparrow} + I_{\uparrow\downarrow}$$
$$I_\downarrow = I_{\downarrow\downarrow} + I_{\downarrow\uparrow}, \qquad (8.7.4.39)$$

which depend only on the polarization of the incident neutron.

#### 8.7.4.4.2. *Unpolarized neutron scattering*

If the incident neutron beam is not polarized, the scattering cross section is given by

$$I = \tfrac{1}{2}[I_\uparrow + I_\downarrow] = |F_N|^2 + |\mathbf{Q}|^2. \qquad (8.7.4.40)$$

Magnetic and nuclear contributions are simply additive. With $x = Q/F_N$, one obtains

$$I = |F_N|^2[1 + |x|^2]. \qquad (8.7.4.41)$$

Owing to its definition, $|x|$ can be of the order of 1 if and only if the atomic moments are ordered close to saturation (as in the ferro- or antiferromagnets). In many situations of structural and chemical interest, $|x|$ is small.

If, for example, $|x| \sim 0.05$, the magnetic contribution in (8.7.4.41) is only 0.002 of the total intensity. Weak magnetic effects, such as occur for instance in paramagnets, are thus hardly detectable with unpolarized neutron scattering.

However, if the magnetic structure does not have the same periodicity as the crystalline structure, magnetic components in (8.7.4.40) occur at scattering vectors for which the nuclear contribution is zero. In this case, the unpolarized technique is of unique interest. Most phase diagrams involving antiferromagnetic or helimagnetic order and modulations of such ordering are obtained by this method.

#### 8.7.4.4.3. *Polarized neutron scattering*

It is generally possible to polarize the incident beam by using as a monochromator a ferromagnetic alloy, for which at a given Bragg angle $I_\downarrow(\text{monochromator}) = 0$, because of a cancellation of nuclear and magnetic scattering components. The scattered-beam intensity is thus $I_\uparrow$. By using a radio-frequency (r.f.) coil tuned to the Larmor frequency of the neutron, the neutron spin can be flipped into the ($\downarrow$) state for which the scattered beam intensity is $I_\downarrow$. This allows measurement of the 'flipping ratio' $R(\mathbf{h})$:

$$R(\mathbf{h}) = \frac{I_\uparrow(\mathbf{h})}{I_\downarrow(\mathbf{h})}. \qquad (8.7.4.42)$$

As the two measurements are made under similar conditions, most systematic effects are eliminated by this technique, which is only applicable to cases where both $F_N$ and $F_M$ occur at the same scattering vectors. This excludes any antiferromagnetic type of ordering.

The experimental set-up is discussed by Forsyth (1980).

#### 8.7.4.4.4. *Polarized neutron scattering of centrosymmetric crystals*

If $\boldsymbol{\lambda}$ is assumed to be in the vertical $Oz$ direction, $\mathbf{M}(\mathbf{h})$ will in most situations be aligned along $Oz$ by an external orienting field. If $\alpha$ is the angle between $\mathbf{M}$ and $\mathbf{h}$, and

$$x = \frac{r_0 M(\mathbf{h})}{F_N(\mathbf{h})}, \qquad (8.7.4.43)$$

with $F_N$ expressed in the same units as $r_0$, one obtains, for centrosymmetric crystals,

$$R = \frac{1 + 2x\sin^2\alpha + x^2\sin^2\alpha}{1 - 2x\sin^2\alpha + x^2\sin^2\alpha}. \qquad (8.7.4.44)$$

If $x \ll 1$,

$$R \sim 1 + 4x\sin^2\alpha. \qquad (8.7.4.45)$$

For $x \sim 0.05$ and $\alpha = \pi/2$, $R$ now departs from 1 by as much as 20%, which proves the enormous advantage of polarized neutron scattering in the case of low magnetism.

Equation (8.7.4.44) can be inverted, and $x$ and its sign can be obtained directly from the observation. However, in order to obtain $M(\mathbf{h})$, the nuclear structure factor $F_N(\mathbf{h})$ must be known, either from nuclear scattering or from a calculation. All systematic errors that affect $F_N(\mathbf{h})$ are transferred to $M(\mathbf{h})$.

For two reasons, it is not in general feasible to access all reciprocal-lattice vectors. First, in order to have reasonable statistical accuracy, only reflections for which both $I_\uparrow$ and $I_\downarrow$ are large enough are measured; *i.e.* reflections having a strong nuclear structure factor. Secondly, $\sin\alpha$ should be as close to 1 as possible, which may prevent one from accessing all directions in reciprocal space. If $\mathbf{M}$ is oriented along the vertical axis, the simplest experiment consists of recording reflections with $\mathbf{h}$ in the horizontal plane, which leads to a projection of $\mathbf{m}(\mathbf{r})$ in real space. When possible, the sample is rotated so that other planes in the reciprocal space can be recorded.

Finally, if $\alpha = \pi/2$, $I_{\uparrow\downarrow}$ vanishes, and neutron spin is conserved in the experiment.

#### 8.7.4.4.5. *Polarized neutron scattering in the noncentrosymmetric case*

If the space group is noncentrosymmetric, both $F_N$ and $M$ have a phase, $\varphi_N$ and $\varphi_M$, respectively.

If for simplicity one assumes $\alpha = \pi/2$, and, defining $\delta = \varphi_M - \varphi_N$,

$$R = \frac{1 + |x|^2 + 2|x|\cos\delta}{1 + |x|^2 - 2|x|\cos\delta}, \qquad (8.7.4.46)$$

which shows that $|x|$ and $\delta$ cannot both be obtained from the experiment.

The noncentrosymmetric case can only be solved by a careful modelling of the magnetic structure factor as described in Subsection 8.7.4.5.

In practice, neither the polarization of the incident beam nor the efficiency of the r.f. flipping coil is perfect. This leads to a modification in the expression for the flipping ratios [see Section 6.1.3 or Forsyth (1980)].

#### 8.7.4.4.6. *Effect of extinction*

Since most measurements correspond to strong nuclear structure factors, extinction severely affects the observed data. To a first approximation, one may assume that both $I_{\uparrow\uparrow}$ and $I_{\downarrow\downarrow}$ will be affected by this process, though the spin-flip processes $I_{\uparrow\downarrow}$ and $I_{\downarrow\uparrow}$ are not. If $y_{\uparrow\uparrow}$ and $y_{\downarrow\downarrow}$ are the associated extinction factors, the observed flipping ratio is

$$R_{\text{obs}} \sim \frac{I_{\uparrow\uparrow}y_{\uparrow\uparrow} + I_{\uparrow\downarrow}}{I_{\downarrow\downarrow}y_{\downarrow\downarrow} + I_{\uparrow\downarrow}}, \qquad (8.7.4.47)$$

where the expressions for $y_{\uparrow\uparrow,\downarrow\downarrow}$ are given elsewhere (Bonnet, Delapalme, Becker & Fuess, 1976).

It should be emphasized that, even in the case of small magnetic structure factors, extinction remains a serious problem since, even though $y_{\uparrow\uparrow}$ and $y_{\downarrow\downarrow}$ may be very close to each other,

so are $I_{\uparrow\uparrow}$ and $I_{\downarrow\downarrow}$. An incorrect treatment of extinction may entirely bias the estimate of $x$.

#### 8.7.4.4.7. *Error analysis*

In the most general case, it is not possible to obtain $x$, and thus $M(\mathbf{h})$ directly from $R$. Moreover, it is unlikely that all Bragg spots within the reflection sphere could be measured. Modelling of $\mathbf{M}(\mathbf{h})$ is thus of crucial importance. The analysis of data must proceed through a least-squares routine fitting $R_{\rm calc}$ to $R_{\rm obs}$, minimizing the error function

$$\varepsilon = \sum_{\substack{\mathbf{h}\\ \text{observed}}} \frac{1}{\sigma^2(R)} [R_{\rm obs}(\mathbf{h}) - R_{\rm calc}(\mathbf{h})]^2, \tag{8.7.4.48}$$

where $R_{\rm calc}$ corresponds to a model and $\sigma^2(R)$ is the standard uncertainty for $R$.

If the same counting time for $I_\uparrow$ and for $I_\downarrow$ is assumed, only the counting statistical error may be considered important in the estimate of $R$, as most systematic effects cancel. In the simple case where $\alpha = \pi/2$, and the structure is centrosymmetric, a straightforward calculation leads to

$$\frac{\sigma^2(x)}{x^2} = \frac{\sigma^2(R)}{R^2} \frac{R}{(R-1)^2}; \tag{8.7.4.49}$$

with

$$\frac{\sigma^2(R)}{R^2} \sim \frac{1}{I_\uparrow} + \frac{1}{I_\downarrow}, \tag{8.7.4.50}$$

one obtains the result

$$\frac{\sigma^2(x)}{x^2} = \tfrac{1}{8} \frac{(F_N^2 + M^2)}{(F_N M)^2}. \tag{8.7.4.51}$$

In the common case where $x \ll 1$, this reduces to

$$\frac{\sigma^2(x)}{x^2} \sim \tfrac{1}{8} \frac{1}{M^2} = \frac{1}{8F_N^2} \frac{1}{x^2}. \tag{8.7.4.52}$$

In addition to this estimate, care should be taken of extinction effects.

The real interest is in $M(\mathbf{h})$, rather than $x$:

$$\frac{\sigma^2(M)}{M^2} = \frac{\sigma^2(x)}{x^2} + \frac{\sigma^2(F_N)}{F_N^2}. \tag{8.7.4.53}$$

If $F_N$ is obtained by a nuclear neutron scattering experiment,

$$\sigma^2(F_N) \sim a + bF_N^2,$$

where $a$ accounts for counting statistics and $b$ for systematic effects.

The first term in (8.7.4.53) is the leading one in many situations. Any systematic error in $F_N$ can have a dramatic effect on the estimate of $M(\mathbf{h})$.

### 8.7.4.5. *Modelling the spin density*

In this subsection, the case of spin-only magnetization is considered. The modelling of $\mathbf{m}_s(\mathbf{r})$ is very similar to that of the charge density.

#### 8.7.4.5.1. *Atom-centred expansion*

We first consider the case where spins are localized on atoms or ions, as it is to a first approximation for compounds involving transition-metal atoms. The magnetization density is expanded as

$$\mathbf{m}_S(\mathbf{r}) = \sum_j \langle \mathbf{S}_j \rangle \, \langle s_j(\mathbf{r} - \mathbf{R}_j) \rangle, \tag{8.7.4.54}$$

where $\langle \mathbf{S}_j \rangle$ is the spin at site $j$, and $\langle s_j \rangle$ the thermally averaged normalized spin density $f_j(\mathbf{h})$, the Fourier transform of $s_j(\mathbf{r})$, is known as the 'magnetic form factor'. Thus,

$$\mathbf{M}(\mathbf{h}) = \sum_j \langle \mathbf{S}_j \rangle \, f_j(\mathbf{h}) \, T_j \exp(2\pi \mathbf{h} \cdot \mathbf{R}_j), \tag{8.7.4.55}$$

where $T_j$ and $\mathbf{R}_j$ are the Debye–Waller factor and the equilibrium position of the $j$th site, respectively.

Most measurements are performed at temperatures low enough to ensure a fair description of $T_j$ at the harmonic level (Coppens, 1992). $T_j$ represents the vibrational relaxation of the open-shell electrons and may, in some situations, be different from the Debye–Waller factor of the total charge density, though at present no experimental evidence to this effect is available.

##### 8.7.4.5.1.1. *Spherical-atom model*

In the crudest model, $s_j(\mathbf{r})$ is approximated by its spherical average. If the magnetic electrons have a wavefunction radial dependence represented by the radial function $U(r)$, the magnetic form factor is given by

$$f(h) = \int_0^\infty U^2(r) 4\pi r^2 \, \mathrm{d}r j_0(2\pi hr) = \langle j_0 \rangle, \tag{8.7.4.56}$$

where $j_0$ is the zero-order spherical Bessel function. For free atoms and ions, these form factors can be found in *IT* IV (1974).

One of the important features of magnetic neutron scattering is the fact that, to a first approximation, closed shells do not contribute to the form factor. Thus, it is a unique probe of the electronic structure of heavy elements, for which theoretical calculations even at the atomic level are questionable. Relativistic effects are important. Theoretical relativistic form factors can be used (Freeman & Desclaux, 1972; Desclaux & Freeman, 1978). It is also possible to parametrize the radial behaviour of $U$. A single contraction-expansion model [$\kappa$ refinement, expression (8.7.3.6)] is easy to incorporate.

##### 8.7.4.5.1.2. *Crystal-field approximation*

Crystal-field effects are generally of major importance in spin magnetism and are responsible for the spin state of the ions, and thus for the ground-state configuration of the system. Thus, they have to be incorporated in the model.

Taking the case of a transition-metal compound, and neglecting small contributions that may arise from spin polarization in the closed shells (see Subsections 8.7.4.9 and 8.7.4.10), the normalized spin density can be written by analogy with (8.7.3.76) as

$$s(\mathbf{r}) = \sum_{i=1}^{5} \sum_{j \geq i}^{5} D_{ij} \, d_i(\mathbf{r}) d_j(\mathbf{r}), \tag{8.7.4.57}$$

where $D_{ij}$ is the normalized spin population matrix. If $\rho_{d\uparrow}$ and $\rho_{d\downarrow}$ are the densities of a given spin,

$$s(\mathbf{r}) = \frac{\rho_{d\uparrow} - \rho_{d\downarrow}}{n_\uparrow - n_\downarrow}, \tag{8.7.4.58}$$

the $d$-type charge density is

$$\rho_d(\mathbf{r}) = \rho_{d\uparrow} + \rho_{d\downarrow} \tag{8.7.4.59}$$

and is expanded in a similar way to $s(\mathbf{r})$ [see (8.7.3.76)],

$$\rho_d(\mathbf{r}) = \sum_i \sum_{j \geq i} P_{ij} d_i d_j; \tag{8.7.4.60}$$

writing

$$\rho_{d\sigma} = \sum P_{ij}^{\sigma} d_i d_j \tag{8.7.4.61}$$

with $\sigma = \uparrow$ and $\downarrow$, one obtains

$$\begin{aligned} P_{ij} &= P_{ij}^{\uparrow} + P_{ij}^{\downarrow} \\ D_{ij} &= (P_{ij}^{\uparrow} - P_{ij}^{\downarrow})/(n_{\uparrow} - n_{\downarrow}). \end{aligned} \tag{8.7.4.62}$$

Similarly to $\rho_d(\mathbf{r})$, $s(r)$ can be expanded as

$$s(\mathbf{r}) = U^2(r) \sum_{l=0}^{4} \sum_{m=0}^{l} \sum_{p} D_{lmp}\, y_{lmp}(\theta, \varphi), \tag{8.7.4.63}$$

where $U(r)$ describes the radial dependence. Spin polarization leads to a further modification of this expression. Since the numbers of electrons of a given spin are different, the exchange interaction is different for the two spin states, and a spin-dependent effective screening occurs. This leads to

$$\rho_{d\sigma}(\mathbf{r}) = \kappa_{\sigma}^3 U^2(\kappa_{\sigma} r) \sum_{lmp} P_{lmp}^{\sigma}\, y_{lmp}, \tag{8.7.4.64}$$

with $\sigma = \uparrow$ or $\downarrow$, where two $\kappa$ parameters are needed.

The complementarity between charge and spin density in the crystal field approximation is obvious. At this particular level of approximation, expansions are exact and it is possible to estimate $d$-orbital populations for each spin state.

#### 8.7.4.5.1.3. *Scaling of the spin density*

The magnetic structure factor is scaled to $F_N(\mathbf{h})$. Whether the nuclear structure factors are calculated from refined structural parameters or obtained directly from a measurement, their scale factor is not rigorously fixed.

As a result, it is not possible to obtain absolute values of the effective spins $\langle \mathbf{S}_n \rangle$ from a magnetic neutron scattering experiment. It is necessary to scale them through the sum rule

$$\sum_{n} \langle \mathbf{S}_n \rangle = \boldsymbol{\mu}, \tag{8.7.4.65}$$

where $\boldsymbol{\mu}$ is the macroscopic magnetization of the sample.

The practical consequences of this constraint for a refinement are similar to the electroneutrality constraint in charge-density analysis (§8.7.3.3.1).

#### 8.7.4.5.2. *General multipolar expansion*

In this subsection, the localized magnetism picture is assumed to be valid. However, each subunit can now be a complex ion or a radical. Covalent interactions must be incorporated.

If $\chi_{\mu}(\mathbf{r})$ are atomic basis functions, the spin density $s(\mathbf{r})$ can always be written as

$$s(\mathbf{r}) = \sum_{\mu} \sum_{\nu} D_{\mu\nu} \chi_{\mu}(\mathbf{r} - \mathbf{R}_{\mu}) \chi_{\nu}(\mathbf{r} - \mathbf{R}_{\nu}), \tag{8.7.4.66}$$

an expansion that is similar to (8.7.3.9) for the charge density.

To a first approximation, only the basis functions that are required to describe the open shell have to be incorporated, which makes the expansion simple and more flexible than for the charge density.

As for the charge density, it is possible to project (8.7.4.66) onto the various sites of the ion or molecule by a multipolar expansion:

$$\begin{aligned} s(\mathbf{r}) &\sim \sum_{j} s_j(\mathbf{r} - \mathbf{R}_j) * P_j(\mathbf{R}_j), \\ s_j(\mathbf{r}) &= \sum_{j} \kappa_j^3 R_{lj}(\kappa_j r) \sum_{m} \sum_{p} D_{jlmp}\, y_{lmp}. \end{aligned} \tag{8.7.4.67}$$

$P(\mathbf{R}_j)$ is the vibrational p.d.f. of the $j$th atom, which implies use of the convolution approximation.

The monopolar terms $D_{j00}$ give an estimate of the amount of spin transferred from a central metal ion to the ligands, or of the way spins are shared among the atoms in a radical.

The constraint (8.7.4.65) becomes

$$\sum_{n} \langle \mathbf{S}_n \rangle \sum_{j} D_{j00}^{(n)} = \boldsymbol{\mu}, \tag{8.7.4.68}$$

where $(n)$ refers to the various subunits in the unit cell. Expansion (8.7.4.67) is the key for solving noncentrosymmetric magnetic structure (Boucherle, Gillon, Maruani & Schweizer, 1982).

#### 8.7.4.5.3. *Other types of model*

One may wish to take advantage of the fact that, to a good approximation, only a few molecular orbitals are involved in $s(\mathbf{r})$. In an independent particle model, one expands the relevant orbitals in terms of atomic basis functions (LCAO):

$$\varphi_{i\sigma} = \sum_{\mu} c_{i\mu}^{\sigma} \chi_{\mu}^{\sigma}(\mathbf{r} - \mathbf{R}_{\mu}) \tag{8.7.4.69}$$

with $\sigma = \uparrow$ or $\downarrow$, and the spin density is expanded according to (8.7.4.21) and (8.7.4.23). Fourier transform of two centre-term products is required. Details can be found in Forsyth (1980) and Tofield (1975).

In the case of extended solids, expansion (8.7.4.69) must refer to the total crystal, and therefore incorporate translational symmetry (Brown, 1986).

Finally, in the simple systems such as transition metals, like Ni, there is a $d$–$s$ type of interaction, leading to some contribution to the spin density from delocalized electrons (Mook, 1966). If $s_l$ and $s_d$ are the localized and delocalized parts of the density, respectively,

$$s(\mathbf{r}) = a s_l(\mathbf{r}) + [1 - a] s_d(\mathbf{r}), \tag{8.7.4.70}$$

where $a$ is the fraction of localized spins. $s_d(\mathbf{r})$ can be modelled as being either constant or a function with a very small number of Fourier adjustable coefficients.

### 8.7.4.6. *Orbital contribution to the magnetic scattering*

$Q_L(\mathbf{h})$ is given by (8.7.4.10) and (8.7.4.12). Since $\nabla\psi$ in (8.7.4.11) does not play any role in the scattering cross section, we can use the restriction

$$\mathbf{j}(\mathbf{r}) = \nabla \times \mathbf{m}_L(\mathbf{r}), \tag{8.7.4.71}$$

where $\mathbf{m}_L(\mathbf{r})$ is defined to an arbitrary gradient. It is possible to constrain $\mathbf{m}_L(\mathbf{r})$ to have the form

$$\mathbf{m}_L(\mathbf{r}) = \hat{\mathbf{r}} \times \mathbf{v}(\mathbf{r}),$$

since any radial component could be considered as the radial component of a gradient. With spherical coordinates, (8.7.4.71) becomes

$$\mathbf{j} = -\frac{1}{r} \frac{\partial}{\partial r} [r\mathbf{v}],$$

which can be integrated as

$$\mathbf{r} \times \mathbf{v} = -\int_{r}^{\infty} y \hat{\mathbf{r}} \times \mathbf{j}(y\hat{\mathbf{r}})\, \mathrm{d}y;$$

one finally obtains

$$\mathbf{m}_L(\mathbf{r}) = \frac{1}{r} \int_{y=r}^{y=\infty} \hat{\mathbf{r}} y \times \mathbf{j}(\hat{\mathbf{r}} y)\, \mathrm{d}y. \tag{8.7.4.72}$$

With $f(x)$ defined by

$$f(x) = -\frac{1}{x^2}\int_0^{ix} tl^t\,\mathrm{d}t, \qquad (8.7.4.73)$$

the expression for $\mathbf{M}_L(\mathbf{h})$ is obtained by Fourier transformation of (8.7.4.72):

$$M_L(\mathbf{h}) = \tfrac{1}{2}\int \mathbf{r}\times\mathbf{j}(\mathbf{r}) f(\mathbf{h}\cdot\mathbf{r})\,\mathrm{d}\mathbf{r},$$

which leads to

$$\mathbf{M}_L(\mathbf{h}) = \tfrac{1}{4}\left\langle \sum_j \left\{ \mathbf{l}_j f(2\pi\mathbf{h}\cdot\mathbf{r}_j) + f(2\pi\mathbf{h}\cdot\mathbf{r}_j)\mathbf{l}_j \right\} \right\rangle \qquad (8.7.4.74)$$

by using the definition (8.7.4.9) of $\mathbf{j}$.

This expression clearly shows the connection between orbital magnetism and the orbital angular momentum of the electrons. It is of general validity, whatever the origin of orbital magnetism.

Since $f(0) = 1$,

$$\mathbf{M}_L(0) = \tfrac{1}{2}\langle\mathbf{L}\rangle, \qquad (8.7.4.75)$$

as expected.

#### 8.7.4.6.1. *The dipolar approximation*

The simplest approximation involves decomposing $\mathbf{j}(\mathbf{r})$ into atomic contributions:

$$\mathbf{j}(\mathbf{r}) = \sum_n \mathbf{j}_n(\mathbf{r}-\mathbf{R}_n). \qquad (8.7.4.76)$$

One obtains

$$\mathbf{M}_L = \sum_n \mathbf{M}_{L,n}(\mathbf{h}) \exp(2\pi i\mathbf{h}\cdot\mathbf{R}_n). \qquad (8.7.4.77)$$

$\mathbf{M}_{L,n}(\mathbf{h})$ is the atomic magnetic orbital structure factor.

We notice that $f(2\pi\mathbf{h}\cdot\mathbf{r})$ as defined in (8.7.4.73) can be expanded as

$$f(2\pi\mathbf{h}\cdot\mathbf{r}) = 4\pi\sum_l\sum_m (i)^l \gamma_l(2\pi hr)\, Y_{lm}(\hat{r})\, Y^*_{lm}(\hat{h}), \qquad (8.7.4.78)$$

where

$$\gamma_l(x) = \frac{2}{x^2}\int_0^x tj_l(t)\,\mathrm{d}t. \qquad (8.7.4.79)$$

$j_l$ is a spherical Bessel function of order $l$, and $Y_{lm}$ are the complex spherical harmonic functions.

If one considers only the spherically symmetric term in (8.7.4.78), one obtains the 'dipolar approximation', which gives

$$\mathbf{M}^D_{L,n} = \tfrac{1}{2}\langle\mathbf{L}_n\rangle\langle\gamma_{0n}\rangle, \qquad (8.7.4.80)$$

with

$$\langle\gamma_{0n}\rangle = \int_0^\infty 4\pi r^2 U_n^2(r)\gamma_0(2\pi hr)\,\mathrm{d}r,$$

and

$$\gamma_0(x) = \frac{2}{x^2}(1-\cos x). \qquad (8.7.4.81)$$

$U_n(r)$ is the radial function of the atomic electrons whose orbital momentum is unquenched. Thus, in the dipolar approximation, the atomic orbital scattering is proportional to the effective orbital angular momentum and therefore to the orbital part of the magnetic dipole moment of the atom.

Within the same level of approximation, the spin structure factor is

$$\mathbf{M}_S = \sum_n \mathbf{M}_{S,n}(\mathbf{h}) \exp(2\pi i\mathbf{h}\cdot\mathbf{R}_n), \qquad (8.7.4.82)$$

with

$$\mathbf{M}_{S,n}(\mathbf{h}) = \langle\mathbf{S}_\mathbf{n}\rangle\langle j_{0n}\rangle,$$

and

$$\langle j_{0n}\rangle = \int_0^\infty 4\pi r^2 U_n^2(r) j_0(2\pi hr)\,\mathrm{d}r.$$

Finally, the atomic contribution to the total magnetic structure factor is

$$\mathbf{M}^D_n = \langle\mathbf{S}_n\rangle\langle j_{0n}\rangle + \tfrac{1}{2}\langle\mathbf{L}_n\rangle\langle\gamma_{0n}\rangle. \qquad (8.7.4.83)$$

If $\langle\mathbf{J}_n\rangle$ is the total angular momentum of atom $n$ and $g_n$ its gyromagnetic ratio, (8.7.4.35)–(8.7.4.37) lead to:

$$\mathbf{M}^D_n = \langle\mathbf{J}_n\rangle\left\{[g_n-1]\langle j_{0n}\rangle + \frac{2-g_n}{2}\langle\gamma_{0n}\rangle\right\}. \qquad (8.7.4.84a)$$

Another approach, which is applicable only to the atomic case, is often used, which is based on Racah's algebra (Marshall & Lovesey, 1971). At the dipolar approximation level, it leads to a slightly different result, according to which $\langle\gamma_{0n}\rangle$ is replaced by

$$\langle\gamma_{0n}\rangle \sim \langle j_{0n}\rangle + \langle j_{2n}\rangle. \qquad (8.7.4.85)$$

The two results are very close for small $\mathbf{h}$ where the dipolar approximation is correct. With (8.7.4.35)–(8.7.4.37), (8.7.4.84*a*) can also be written as

$$\mathbf{M}^D_n = \mathbf{M}^D_{S,n} + \langle\mathbf{S}_n\rangle\frac{2-g_n}{2(g_n-1)}\langle\gamma_{0n}\rangle, \qquad (8.7.4.84b)$$

where the second term is the 'orbital correction'. Its magnitude clearly depends on the difference between $g_n$ and 2, which is small in 3*d* elements but can become important for rare earths.

#### 8.7.4.6.2. *Beyond the dipolar approximation*

Expressions (8.7.4.74) and (8.7.4.78) are valid in any situation where orbital scattering occurs. They can in principle be used to estimate from the diffraction experiment the contribution of a few configurations that interact due to the $\mathbf{L}\cdot\mathbf{S}$ operator. In delocalized situations, (8.7.4.74) is the most suitable approach, while Racah's algebra can only be applied to one-centre cases.

#### 8.7.4.6.3. *Electronic structure of rare-earth elements*

When covalency is small, the major aims are the determination of the ground state of the rare-earth ion, and the amount of delocalized magnetization density *via* the conduction electrons.

The ground state $|\psi\rangle$ of the ion is written as

$$|\psi\rangle = \sum_M a_M|JM\rangle, \qquad (8.7.4.86)$$

which is well suited for the Johnston (1966) and Marshall–Lovesey (1971) formulation in terms of general angular-momentum algebra. A multipolar expansion of spin and orbital components of the structure factor enables a determination of the expansion coefficient $a_M$ (Schweizer, 1980).

### 8.7.4.7. *Properties derivable from spin densities*

The derivation of electrostatic properties from the charge density was treated in Subsection 8.7.3.4. Magnetostatic properties can be derived from the spin-magnetization density $\mathbf{m}_s(\mathbf{r})$ using parallel expressions.

8.7.4.7.1. *Vector fields*

The vector potential field is defined as

$$\mathbf{A}(\mathbf{r}) = \int \frac{\mathbf{m}_s(\mathbf{r}') \times (\mathbf{r} - \mathbf{r}')}{|\mathbf{r} - \mathbf{r}'|^3} \, \mathrm{d}\mathbf{r}'. \quad (8.7.4.87)$$

In the case of a crystal, it can be expanded in Fourier series:

$$\mathbf{A}(\mathbf{r}) = \frac{2i}{V} \sum_{\mathbf{h}} \left\{ \frac{\mathbf{M}_S(\mathbf{h}) \times \mathbf{h}}{h^2} \right\} \exp(-2\pi i \mathbf{h} \cdot \mathbf{r}); \quad (8.7.4.88)$$

the magnetic field is simply

$$\begin{aligned} \mathbf{B}(\mathbf{r}) &= \boldsymbol{\nabla} \times \mathbf{A}(\mathbf{r}) \\ &= -\frac{4\pi}{V} \sum_{\mathbf{h}} \left[ \frac{\mathbf{h} \times \mathbf{M}_S(\mathbf{h}) \times \mathbf{h}}{h^2} \right] \exp(-2\pi i \mathbf{h} \cdot \mathbf{r}). \end{aligned} \quad (8.7.4.89)$$

One notices that there is no convergence problem for the $\mathbf{h} = 0$ term in the $\mathbf{B}(\mathbf{r})$ expansion.

The magnetostatic energy, *i.e.* the amount of energy that is required to obtain the magnetization $\mathbf{m}_s$, is

$$\begin{aligned} E_{ms} &= -\tfrac{1}{2} \int_{\text{cell}} \mathbf{m}_s(\mathbf{r}) \cdot \mathbf{B}(\mathbf{r}) \, \mathrm{d}r \\ &= \frac{2\pi}{V} \sum_{\mathbf{h}} \frac{[\mathbf{M}_s(-\mathbf{h}) \times \mathbf{h}] \cdot [\mathbf{M}_S(\mathbf{h}) \times \mathbf{h}]}{h^2}. \end{aligned} \quad (8.7.4.90)$$

It is often interesting to look at the magnetostatics of a given subunit: for instance, in the case of paramagnetic species.

For example, the vector potential outside the magnetized system can be obtained in a similar way to the electrostatic potential (8.7.3.30):

$$\mathbf{A}(\mathbf{r}') = \int \frac{[\boldsymbol{\nabla} \times \mathbf{m}_S(\mathbf{r})]}{|\mathbf{r} - \mathbf{r}'|} \, \mathrm{d}\mathbf{r}. \quad (8.7.4.91)$$

If $r' \gg r$, $1/|\mathbf{r} - \mathbf{r}'|$ can be easily expanded in powers of $1/r'$, and $\mathbf{A}(\mathbf{r}')$ can thus be obtained in powers of $1/r'$. If $\mathbf{m}_s(\mathbf{r}) = \langle \mathbf{S} \rangle s(\mathbf{r})$,

$$\mathbf{A}(\mathbf{r}') = \langle \mathbf{S} \rangle \times \int \frac{\boldsymbol{\nabla} s(\mathbf{r})}{|\mathbf{r} - \mathbf{r}'|} \, \mathrm{d}\mathbf{r}. \quad (8.7.4.92)$$

8.7.4.7.2. *Moments of the magnetization density*

Among the various properties that are derivable from the delocalized spin density function, the dipole coupling tensor is of particular importance:

$$D_{nij}(\mathbf{R}_n) = \int s(\mathbf{r}) \frac{[3 r_{ni} r_{nj} - r_n^2 \delta_{ij}]}{r_n^5} \, \mathrm{d}\mathbf{r}, \quad (8.7.4.93)$$

where $\mathbf{R}_n$ is a nuclear position and $\mathbf{r}_n = \mathbf{r} - \mathbf{R}_n$. This dipolar tensor is involved directly in the hyperfine interaction between a nucleus with spin $\mathbf{I}_n$ and an electronic system with spin $\mathbf{s}$, through the interaction energy

$$\sum_{i,j} I_{ni} D_{nij} S_j. \quad (8.7.4.94)$$

This tensor is measurable by electron spin resonance for either crystals or paramagnetic species trapped in matrices. The complementarity with scattering is thus of strong importance (Gillon, Becker & Ellinger, 1983).

Computational aspects are the same as in the electric field gradient calculation, $\rho(\mathbf{r})$ being simply replaced by $s(\mathbf{r})$ (see Subsection 8.7.3.4).

8.7.4.8. *Comparison between theory and experiment*

Since it is a measure of the imbalance between the densities associated with the two spin states of the electron, the spin-density function is a probe that is very sensitive to the exchange forces in the system. In an independent-particle model (Hartree–Fock approximation), the exchange mean field potential involves exchange between orbitals with the same spin. Therefore, if the numbers of ↑ and ↓ spins are different, one expects $V_{\text{exch}}\uparrow$ to be different from $V_{\text{exch}}\downarrow$. The main consequence of this is the necessity to solve two different Fock equations, one for each spin state. This is known as the spin-polarization effect: starting from a paired orbital, a slight spatial decoupling arises from this effect, and closed shells do have a participation in the spin density.

It can be shown that this effect is hardly visible in the charge density, but is enhanced in the spin density.

Spin densities are a very good probe for calculations involving this spin-polarization effect: The unrestricted Hartree–Fock approximation (Gillon, Becker & Ellinger, 1983).

From a common spin-restricted approach, spin polarization can be accounted for by a mixture of Slater determinants (configuration interaction), where the configuration interaction is only among electrons with the same spin. There is also a correlation among electrons with different spins, which is more difficult to describe theoretically. There seems to be evidence for such effects from comparison of experimental and theoretical spin densities in radicals (Delley, Becker & Gillon, 1984), where the unrestricted Hartree–Fock approximation is not sufficient to reproduce experimental facts. In such cases, local-spin-density functional theory has revealed itself very satisfactorily. It seems to offer the most efficient way to include correlation effects in spin-density functions.

As noted earlier, analysis of the spin-density function depends more on modelling than that of the charge density. Therefore, in general, 'experimental' spin densities at static densities and the problem of theoretical averaging is minor here. Since spin density involves essentially outer-electron states, resolution in reciprocal space is less important, except for analysis of the polarization of the core electrons.

8.7.4.9. *Combined charge- and spin-density analysis*

Combined charge- and spin-density analysis requires performing X-ray and neutron diffraction experiments at the same temperature. Magnetic neutron experiments are often only feasible around 4 K, and such conditions are more difficult to achieve by X-ray diffraction. Even if the two experiments are to be performed at different temperatures, it is often difficult to identify compounds suitable for both experiments.

Owing to the common parametrization of $\rho(\mathbf{r})$ and $s(\mathbf{r})$, a combined least-squares-refinement procedure can be implemented, leading to a description of $\rho_\uparrow(\mathbf{r})$ and $\rho_\downarrow(\mathbf{r})$, the spin-dependent electron densities. Covalency parameters are obtainable together with spin polarization effects in the closed shells, by allowing $\rho_\uparrow$ and $\rho_\downarrow$ to have different radial behaviour.

Spin-polarization effects would be difficult to model from the spin density alone. But the arbitrariness of the modelling is strongly reduced if both $\rho$ and $s$ are analysed at the same time (Becker & Coppens, 1985; Coppens, Koritszansky & Becker, 1986).

8.7.4.10. *Magnetic X-ray scattering separation between spin and orbital magnetism*

8.7.4.10.1. *Introduction*

In addition to the usual Thomson scattering (charge scattering), there is a magnetic contribution to the X-ray amplitude (de Bergevin & Brunel, 1981; Blume, 1985; Brunel & de Bergvin, 1981; Blume & Gibbs, 1988). In units of the chemical radius $r_e$ of the electron, the total scattering amplitude is

$$A_x = F_C + F_M, \tag{8.7.4.95}$$

where $F_C$ is the charge contribution, and $F_M$ the magnetic part.

Let $\hat{\boldsymbol{\varepsilon}}$ and $\hat{\boldsymbol{\varepsilon}}'$ be the unit vectors along the electric field in the incident and diffracted direction, respectively. $\mathbf{k}$ and $\mathbf{k}'$ denote the wavevectors for the incident and diffracted beams. With these notations,

$$F_C = F(\mathbf{h})\,\hat{\boldsymbol{\varepsilon}} \cdot \hat{\boldsymbol{\varepsilon}}', \tag{8.7.4.96}$$

where $F(\mathbf{h})$ is the usual structure factor, which was discussed in Section 8.7.3 [see also Coppens (1992)].

$$F_M = -i\,\frac{h\omega}{mc^2}\,\{\mathbf{M}_L(\mathbf{h}) \cdot \mathbf{A} + \mathbf{M}_S(\mathbf{h}) \cdot \mathbf{B}\}. \tag{8.7.4.97}$$

$\mathbf{M}_L$ and $\mathbf{M}_S$ are the orbital and spin-magnetization vectors in reciprocal space, and $\mathbf{A}$ and $\mathbf{B}$ are vectors that depend in a rather complicated way on the polarization and the scattering geometry:

$$\begin{aligned}\mathbf{A} &= 4\sin^2\theta\,\hat{\boldsymbol{\varepsilon}} \times \hat{\boldsymbol{\varepsilon}}' - (\hat{\mathbf{k}} + \hat{\mathbf{k}})(\hat{\mathbf{k}} \cdot \hat{\boldsymbol{\varepsilon}}') + (\hat{\mathbf{k}}' \times \hat{\boldsymbol{\varepsilon}}')(\hat{\mathbf{k}}' \cdot \hat{\boldsymbol{\varepsilon}})\\ \mathbf{B} &= \hat{\boldsymbol{\varepsilon}}' \times \hat{\boldsymbol{\varepsilon}} + (\mathbf{k}' + \boldsymbol{\varepsilon}')(\mathbf{k} \cdot \boldsymbol{\varepsilon}) - (\hat{\mathbf{k}} \times \hat{\boldsymbol{\varepsilon}})(\hat{\mathbf{k}} \cdot \hat{\boldsymbol{\varepsilon}}')\\ &\quad - (\hat{\mathbf{k}}' \times \hat{\boldsymbol{\varepsilon}}') \times (\hat{\mathbf{k}} \times \hat{\boldsymbol{\varepsilon}}).\end{aligned} \tag{8.7.4.98}$$

For comparison, the magnetic neutron scattering amplitude can be written in the form

$$F_M^{\text{neutron}} = [\mathbf{M}_L(\mathbf{h}) + M_S(\mathbf{h})] \cdot \mathbf{C}, \tag{8.7.4.99}$$

with $\mathbf{C} = \hat{\mathbf{h}} \times \boldsymbol{\sigma} \times \hat{\mathbf{h}}$.

From (8.7.4.99), it is clear that spin and orbital contributions cannot be separated by neutron scattering. In contrast, the polarization dependencies of $\mathbf{M}_L$ and $\mathbf{M}_S$ are different in the X-ray case. Therefore, owing to the well defined polarization of synchrotron radiation, it is in principle possible to separate experimentally spin and orbital magnetization.

However, the prefactor $(h\omega/mc^2) \sim 10^{-2}$ makes the magnetic contributions weak relative to charge scattering. Moreover, $F_C$ is roughly proportional to the total number of electrons, and $F_M$ to the number of unpaired electrons. As a result, one expects $|F_M/F_C|$ to be about $10^{-3}$.

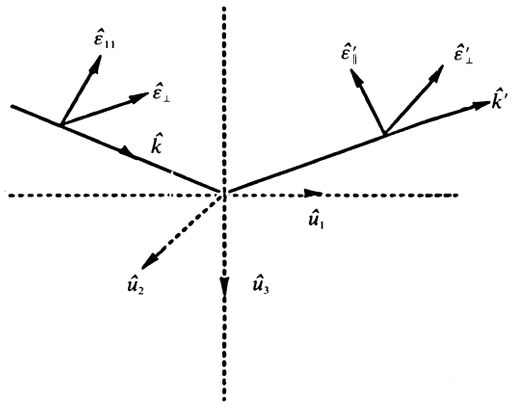


Fig. 8.7.4.1. Some geometrical definitions.

It should also be pointed out that $F_M$ is in quadrature with $F_C$. In many situations, the total X-ray intensity is therefore

$$I_x = |F_C|^2 + |F_M|^2.$$

Thus, under these conditions, the magnetic effect is typically $10^{-6}$ times the X-ray intensity.

Magnetic contributions can be detected if magnetic and charge scattering occur at different positions (antiferromagnetic type of ordering). Furthermore, Blume (1985) has pointed out that the photon counting rate for $|F_M|^2$ at synchrotron sources is of the same order as the neutron rate at high-flux reactors.

Finally, situations where the 'interference' $F_C F_M$ term is present in the intensity are very interesting, since the magnetic contribution becomes $10^{-3}$ times the charge scattering.

The polarization dependence will now be discussed in more detail.

8.7.4.10.2. *Magnetic X-ray structure factor as a function of photon polarization*

Some geometrical definitions are summarized in Fig. 8.7.4.1, where parallel ($\parallel$) and perpendicular ($\perp$) polarizations will be chosen in order to describe the electric field of the incident and diffracted beams. In this two-dimensional basis, vectors $\mathbf{A}$ and $\mathbf{B}$ of (8.7.4.98) can be written as $(2 \times 2)$ matrices:

$$\mathbf{A} = \sin^2\theta \begin{pmatrix} 0 & -(\hat{\mathbf{k}} + \hat{\mathbf{k}}') \\ (\hat{\mathbf{k}} + \hat{\mathbf{k}}') & 2(\hat{\mathbf{k}} \times \hat{\mathbf{k}}') \end{pmatrix} \begin{matrix} \perp \\ \parallel \end{matrix}$$

$$i \rightarrow \quad \perp \qquad\qquad \parallel \qquad\qquad \uparrow f$$

($i$ and $f$ refer to the incident and diffracted beams, respectively);

$$\mathbf{B} = \begin{pmatrix} \hat{\mathbf{k}} \times \hat{\mathbf{k}}' & -2\hat{\mathbf{k}}' \sin^2\theta \\ 2\hat{\mathbf{k}} \sin^2\theta & \hat{\mathbf{k}} \times \hat{\mathbf{k}}' \end{pmatrix}. \tag{8.7.4.100}$$

By comparison, for the Thomson scattering,

$$\hat{\boldsymbol{\varepsilon}} \cdot \hat{\boldsymbol{\varepsilon}}' = \begin{pmatrix} 1 & 0 \\ 0 & \cos 2\theta \end{pmatrix}. \tag{8.7.4.101}$$

The major difference with Thomson scattering is the occurrence of off-diagonal terms, which correspond to scattering processes with a change of polarization. We obtain for the structure factors $A_{if}$:

$$\begin{aligned} A_{\perp\perp} &= F - i\,\frac{\hbar\omega}{mc^2}(\hat{\mathbf{k}} \times \hat{\mathbf{k}}') \cdot \mathbf{M}_S\\ A_{\perp\parallel} &= -2i\,\frac{\hbar\omega}{mc^2}\sin^2\theta\{(\hat{\mathbf{k}} + \hat{\mathbf{k}}') \cdot \mathbf{M}_L + \hat{\mathbf{k}}' \cdot \mathbf{M}_S\}\\ A_{\parallel\perp} &= 2i\,\frac{\hbar\omega}{mc^2}\sin 2\theta\{(\hat{\mathbf{k}} + \hat{\mathbf{k}}') \cdot \mathbf{M}_L + \hat{\mathbf{k}}' \cdot \mathbf{M}_S\}\\ A_{\parallel\parallel} &= F\cos^2\theta - i\,\frac{\hbar\omega}{mc^2}\,(\hat{\mathbf{k}} \times \hat{\mathbf{k}}') \cdot \{4\sin^2\theta\,\mathbf{M}_L\mathbf{M}_S\}. \end{aligned} \tag{8.7.4.102}$$

For a linear polarization, the measured intensity in the absence of diffracted-beam polarization analysis is

$$I_\alpha = |A_{\perp\perp}\cos\alpha + A_{\parallel\perp}\sin\alpha|^2 + |A_{\perp\parallel}\cos\alpha + A_{\parallel\parallel}\sin\alpha|^2, \tag{8.7.4.103}$$

where $\alpha$ is the angle between $\mathbf{E}$ and $\hat{\boldsymbol{\varepsilon}}$. In the centrosymmetric system, without anomalous scattering, no interference term occurs in (8.7.4.103). However, if anomalous scattering is present, $F = F' + iF''$, and terms involving $F''M_S$ or $F''M_L$ appear in the intensity expression.

The radiation emitted in the plane of the electron or positron orbit is linearly polarized. The experimental geometry is

generally such that $(\hat{\mathbf{k}}, \hat{\mathbf{k}}')$ is a vertical plane. Therefore, the polarization of the incident beam is along $\hat{\boldsymbol{\varepsilon}}$ ($\alpha = 0$). If a diffracted-beam analyser passes only $\parallel$ components of the diffracted beam, one can measure $|A_{\perp\parallel}|^2$, and thus eliminate the charge scattering.

For non-polarized radiation (with a rotating anode, for example), the intensity is

$$I = \tfrac{1}{2}[|A_{\parallel\parallel}|^2 + |A_{\parallel\perp}|^2 + |A_{\perp\parallel}|^2 + |A_{\perp\perp}|^2]. \qquad (8.7.4.104)$$

The radiation emitted out of the plane of the orbit contains an increasing amount of circularly polarized radiation. There also exist experimental devices that can produce circularly polarized radiation. For such incident radiation,

$$E_\parallel = \pm iE_\perp \qquad (8.7.4.105)$$

for left- or right-polarized photons. If $\mathbf{E}'$ is the field for the diffracted photons,

$$\begin{aligned} E'_\perp &= A_{\perp\perp} + iA_{\parallel\perp} \\ E'_\parallel &= A_{\parallel\perp} + iA_{\parallel\parallel}. \end{aligned} \qquad (8.7.4.106)$$

In this case, 'mixed-polarization' contributions are in phase with $F$, leading to a strong interference between charge and magnetic scattering.

The case of radiation with a general type of polarization is more difficult to analyse. The most elegant formulation involves Stokes vectors to represent the state of polarization of the incident and scattered radiation (see Blume & Gibbs, 1988).

**Acknowledgements**

Support of this work by the National Science Foundation (CHE8711736 and CHE9615586) is gratefully acknowledged.

**8.6 (*cont.*)**

Von Dreele, R. B. (1997). *Quantitative texture analysis by Rietveld refinement*. *J. Appl. Cryst.* **30**, 517–525.

Von Dreele, R. B., Jorgensen, J. D. & Windsor, C. G. (1982). *Rietveld refinement with spallation neutron powder diffraction data*. *J. Appl Cryst.* **15**, 581–589.

Werner, P. E. (2002). *Autoindexing. Structure determination from powder diffraction data. IUCr Monographs on Crystallography*, No. 13, edited by W. I. F. David, K. Shankland, L. B. McCusker & Ch. Baerlocher, pp. 118–135. Oxford University Press.

Will, G., Parrish, W. & Huang, T. C. (1983). *Crystal structure refinement by profile fitting and least-squares analysis of powder diffractometer data*. *J. Appl Cryst.* **16**, 611–622.

Young, R. A. (1993). Editor. *The Rietveld method. IUCr Monographs on Crystallography,* No. 5. Oxford University Press.

Young, R. A. & Wiles, D. B. (1982). *Profile shape functions in Rietveld refinements*. *J. Appl. Cryst.* **15**, 430–438.

**8.7**

Becker, P. (1990). *Electrostatic properties from X-ray structure factors*. Unpublished results.

Becker, P. & Coppens, P. (1985). *About the simultaneous interpretation of charge and spin density data*. *Acta Cryst.* A**41**, 177–182.

Becker, P. & Coppens, P. (1990). *About the Coulombic potential in crystals*. *Acta Cryst.* A**46**, 254–258.

Bentley, J. (1981). In *Chemical Applications of Atomic and Molecular Electrostatic Potentials*, edited by P. Politzer & D. G. Truhlar. New York/London: Plenum Press.

Bergevin, F. de & Brunel, M. (1981). *Diffraction of X-rays by magnetic materials. I. General formulae and measurements on ferro- and ferrimagnetic compounds*. *Acta Cryst.* A**37**, 314–324.

Bertaut, E. F. (1978). *Electrostatic potentials, fields and gradients*. *J. Phys. Chem. Solids*, **39**, 97–102.

Blume, M. (1985). *Magnetic scattering of X-rays*. *J. Appl. Phys.* **57**, 3615–3618.

Blume, M. & Gibbs, D. (1988). *Polarization dependence of magnetic X-ray scattering*. *Phys. Rev. B*, **37**, 1779–1789.

Bonnet, M., Delapalme, A., Becker, P. & Fuess, H. (1976). *Polarized neutron diffraction – a tool for testing extinction models: application to yttrium iron garnet*. *Acta Cryst.* A**32**, 945–953.

Boucherle, J. X., Gillon, B., Maruani, J. & Schweizer, J. (1982). *Spin densities in centrally unsymmetric structures*. *J. Phys.* (*Paris*) *Colloq.* **7**, 227–230.

Boyd, R. J. (1977). *The radial density function for the neutral atoms from helium to xenon*. *Can. J. Phys.* **55**, 452–455.

Brown, P. J. (1986). *Interpretation of magnetization density measurements in concentrated magnetic systems: exploitation of the crystal translational symmetry*. *Chem. Scr.* **26**, 433–439.

Brunel, M. & de Bergevin, F. (1981). *Diffraction of X-rays by magnetic materials. II. Measurements on antiferromagnetic* $Fe_2O_3$. *Acta Cryst.* A**37**, 324–331.

Buckingham, A. D. (1959). *Molecular quadrupole moments*. *Q. Rev. Chem. Soc.* **13**, 183–214.

Buckingham, A. D. (1970). *Physical chemistry. An advanced treatise*, Vol. 4. *Molecular properties*, edited by D. Henderson, pp. 349–386. New York: Academic Press.

Condon, E. U. & Shortley, G. H. (1935). *The theory of atomic spectra*. Cambridge University Press.

Coppens, P. (1992). *The structure factor. International tables for crystallography*, Vol. B, edited by U. Shmueli, ch. 1.2. Dordrecht: Kluwer Academic Publishers.

Coppens, P., Koritsanszky, T. & Becker, P. (1986). *Transition metal complexes: what can we learn by combining experimental spin and charge densities?* *Chem. Scr.* **26**, 463–467.

Cromer, D. T., Larson, A. C. & Stewart, R. F. (1976). *Crystal structure refinements with generalized scattering factors*. *J. Chem. Phys.* **65**, 336–349.

Cruickshank, D. W. J. (1949). *The accuracy of electron density maps in X-ray analysis with special reference to dibenzyl*. *Acta Cryst.* **2**, 65–82.

Dahl, J. P. & Avery, J. (1984). *Local density approximations in quantum chemsitry and solid state physics*. New York/London: Plenum.

Delley, B., Becker, P. & Gillon, B. (1984). *Local spin-density theory of free radicals: nitroxides*. *J. Chem. Phys.* **80**, 4286–4289.

Desclaux, J. P. & Freeman, A. J. (1978). *J. Magn. Magn. Mater.* **8**, 119–129.

Epstein, J. & Swanton, D. J. (1982). *Electric field gradients in imidazole at 103K from X-ray diffraction*. *J. Chem. Phys.* **77**, 1048–1060.

Fermi, E. (1928). *Eine statitische Methode zur Bestimmung einiger Eigenschaften des Atoms und ihre Anwendung auf die Theorie des periodischen Systems der Elemente*. *Z. Phys.* **48**, 73–79.

Forsyth, J. B. (1980). In *Electron and magnetization densities in molecules and solids*, edited by P. Becker. New York/London: Plenum.

Freeman, A. J. & Desclaux, J. P. (1972). *Neutron magnetic form factor of gadolinium*. *Int. J. Magn.* **3**, 311–317.

Gillon, B., Becker, P. & Ellinger, Y. (1983). *Theoretical spin density in nitroxides. The effect of alkyl substitutions*. *Mol. Phys.* **48**, 763–774.

Gordon, R. G. & Kim, Y. S. (1972). *Theory for the forces between closed-shell atoms and molecules*. *J. Chem. Phys.* **56**, 3122–3133.

Hamilton, W. C. (1964). *Statistical methods in physical sciences*. New York: Ronald Press.

Hellner, E. (1977). *A simple refinement of density distributions of bonding electrons*. *Acta Cryst.* B**33**, 3813–3816.

Hirshfeld, F. L. (1984). *Hellmann–Feynman constraint on charge densities, an experimental test*. *Acta Cryst.* B**40**, 613–615.

Hirshfeld, F. L. & Rzotkiewicz, S. (1974). *Electrostatic binding in the first-row AH and* $A_2$ *diatomic molecules*. *Mol. Phys.* **27**, 1319–1343.

Hirshfelder, J. O., Curtis, C. F. & Bird, R. B. (1954). *Molecular theory of gases and liquids*. New York: John Wiley.

Hohenberg, P. & Kohn, W. (1964). *Inhomogeneous electron gas*. *Phys. Rev. B*, **136**, 864–867.

Holladay, A., Leung, P. C. & Coppens, P. (1983). *Generalized relation between d-orbital occupancies of transition-metal atoms and electron-density multipole population parameters from X-ray diffraction data*. *Acta Cryst.* A**39**, 377–387.

*International Tables for Crystallography* (1992). Vol. B, edited by U. Shmueli. Dordrecht: Kluwer Academic Publishers.

*International Tables for X-ray Crystallography* (1974). Vol. IV. Birmingham: Kynoch Press. (Present distributor: Kluwer Academic Publishers, Dordrecht.)

Johnston, D. F. (1966). *Theory of the electron contribution to the scattering of neutrons by magnetic ions in crystals*. *Proc. Phys. Soc. London*, **88**, 37–52.

Levine, I. L. (1983). *Quantum chemistry*, 3rd ed. Boston/London/Sydney: Allyn and Bacon Inc.

Lovesey, S. W. (1984). *Theory of neutron scattering from condensed matter*. Oxford: Clarendon Press.

Marshall, W. & Lovesey, S. W. (1971). *Theory of thermal neutron scattering*. Oxford University Press.

Massa, L., Goldberg, M., Frishberg, C., Boehme, R. F. & La Placa, S. J. (1985). *Wave functions derived by quantum modeling of the electron density from coherent X-ray diffraction: beryllium metal*. *Phys. Rev. Lett.* **55**, 622–625.

Miller, K. J. & Krauss, M. (1967). *Born inelastic differential cross sections in $H_2$*. *J. Chem. Phys.* **47**, 3754–3762.

Mook, H. A. (1966). *Magnetic moment distribution of Ni metal*. *Phys. Rev.* **148**, 495–501.

Moss, G. & Coppens, P. (1981). *Pseudomolecular electrostatic potentials from X-ray diffraction data*. In *Molecular electrostatic potentials in chemistry and biochemistry*, edited by P. Politzer & D. Truhlar. New York: Plenum.

Pawley, G. S. & Willis, B. T. M. (1970). *Temperature factor of an atom in a rigid vibrating molecule. II. Anisotropic thermal motion*. *Acta Cryst.* A**36**, 260–262.

Rees, B. (1976). *Variance and covariance in experimental electron density studies, and the use of chemical equivalence*. *Acta Cryst.* A**32**, 483–488.

Rees, B. (1978). *Errors in deformation-density and valence-density maps: the scale-factor contribution*. *Acta Cryst.* A**34**, 254–256.

Schweizer, J. (1980). In *Electron and magnetization densities in molecules and crystals*, edited by P. Becker. New York: Plenum.

Spackman, M. A. (1992). *Molecular electric moments from X-ray diffraction data*. *Chem. Rev.* **92**, 1769.

Stevens, E. D. & Coppens, P. (1976). *A priori estimates of the errors in experimental electron densities*. *Acta Cryst.* A**32**, 915–917.

Stevens, E. D., DeLucia, M. L. & Coppens, P. (1980). *Experimental observation of the effect of crystal field splitting on the electron density distribution of iron pyrite*. *Inorg. Chem.* **19**, 813–820.

Stevens, E. D., Rees, B. & Coppens, P. (1977). *Calculation of dynamic electron distributions from static molecular wave functions*. *Acta Cryst.* A**33**, 333–338.

Stewart, R. F. (1977). *One-electron density functions and many-centered finite multipole expansions*. *Isr. J. Chem.* **16**, 124–131.

Stewart, R. F. (1979) *On the mapping of electrostatic properties from Bragg diffraction data*. *Chem. Phys. Lett.* **65**, 335–342.

Su, Z. & Coppens, P. (1992). *On the mapping of electrostatic properties from the multipole description of the charge density*. *Acta Cryst.* A**48**, 188–197.

Su, Z. & Coppens, P. (1994*a*). *Rotation of real spherical harmonics*. *Acta Cryst.* A**50**, 636–643.

Su, Z. & Coppens, P. (1994*b*). *On the evaluation of integrals useful for calculating the electrostatic potential and its derivatives from pseudo-atoms*. *J. Appl. Cryst.* **27**, 89–91.

Thomas, L. H. (1926). *Proc. Cambridge Philos. Soc.* **23**, 542–548.

Tofield, B. C. (1975). *Structure and bonding*, Vol. 21. Berlin: Springer-Verlag.

Ando, Y., Ichimiya, A. & Uyeda, R. (1974). *A determination of values and signs of the 111 and 222 structure factors of silicon*. *Acta Cryst.* A**30**, 600–601.

Bird, D. M. (1990). *Absorption in high-energy electron diffraction from non-centrosymmetric crystals*. *Acta Cryst.* A**46**, 208–214.

Bird, D. M. & King, Q. A. (1990). *Absorption form factors for high-energy electron diffraction*. *Acta Cryst.* A**46**, 202–208.

Bird, D. M. & Saunders, M. (1992). *Sensitivity and accuracy of CBED pattern matching*. *Ultramicroscopy*, **45**, 241–252.

Blackman, M. (1939). *Intensities of electron diffraction rings*. *Proc. R. Soc. London Ser A*, **173**, 68–82.

Burgess, W. G., Preston, A. R., Botton, G. A., Zaluzec, N. J. & Humphreys, C. J. (1994). *Benefits of energy filtering for advanced convergent beam electron diffraction patterns*. *Ultramicroscopy*, **55**, 276–283.

Cowley, J. M. (1992). *Electron diffraction techniques*, Vol. 1. Oxford University Press.

Deininger, C., Necker, G. & Mayer, J. (1994). *Determination of structure factors, lattice strains and accelerating voltage by energy-filtered electron diffraction*. *Ultramicroscopy*, **54**, 15–30.

Fox, A. G. & Fisher, R. M. (1988). *A summary of low-angle X-ray atomic scattering factors measured by the critical voltage effect in high energy electron diffraction*. *Aust. J. Phys.* **41**, 461–468.

Fox, A. G. & Tabbernor, M. A. (1991). *The bonding charge density of $\beta'$ NiAl*. *Acta Metall.* **39**, 669–678.

Gjønnes, J. & Høier, R. (1971). *The application of non-systematic many-beam dynamic effects to structure-factor determination*. *Acta Cryst.* A**27**, 313–316.

Gjønnes, K. & Bøe, N. (1994). *Refinement of temperature factors and charge distributions in $YBa_2Cu_3O_7$ and $YBa_2(Cu,Co)_3O_7$ from CBED intensities*. *Micron Microsc. Acta*, **25**, 29–44.

Gjønnes, K., Gjønnes, J., Zuo, J. & Spence, J. C. H. (1988). *Two-beam features in electron diffraction patterns – application to refinement of low-order structure factors in GaAs*. *Acta Cryst.* A**44**, 810–820.

Goodman, P. & Lehmpfuhl, G. (1967). *Electron diffraction study of MgO h00 systematic interactions*. *Acta Cryst.* **22**, 14–24.

Høier, R., Bakken, L. N., Marthinsen, K. & Holmestad, R. (1993). *Structure factor determination in non-centrosymmetrical crystals by a two-dimensional CBED-based multi-parameter refinement method*. *Ultramicroscopy*, **49**, 159–170.

Høier, R. & Marthinsen, K. (1983). *Effective structure factors in many-beam X-ray diffraction – use of the second Bethe approximation*. *Acta Cryst.* A**39**, 854–860.

Holmestad, R., Krivanek, O. L., Høier, R., Marthinsen, K. & Spence, J. C. H. (1993). *Commercial spectrometer modifications for energy filtering of diffraction patterns and images*. *Ultramicroscopy*, **52**, 454–458.

Holmestad, R., Weickenmeier, A. L., Zuo, J. M., Spence, J. C. H. & Horita, Z. (1993). *Debye–Waller factor measurement in TiAl from HOLZ reflections*. *Electron Microscopy and Analysis 1993*, pp. 141–144. Bristol: IOP Publishing.

Lehmpfuhl, G. (1974). *Dynamical interaction of electron waves in a perfect single crystal*. *Z. Naturforsch. Teil A*, **27**, 424–433.